OTKA-K 101218

FINAL REPORT

Revealing the first eukaryotic nicotinic acid utilization system in the model organism *Aspergillus nidulans*

Zsuzsanna Hamari PhD
University of Szeged
Department of Microbiology

21.01.2016

Abbreviations:
allp: allopurinol
hx: hypoxanthine
N-source: nitrogen source
N-starvation: nitrogen starvation
NA: nicotinic acid
6-NA: 6-hydroxynicotinic acid
4-NQO: 4-nitroquinoline 1-oxide
MOCO: pyranopterin-molybdenum cofactor common to xanthine dehydrogenase
ND: nicotinic acid degradation
NDC: nicotinic acid degradation cluster
NDP: nicotinic acid degradation pathway
PHI: purine hydroxylase I
PHII: purine hydroxylase II
UHP: unknown hydroxylation product
XDH: xanthine dehydrogenase
WT: wild type

Summary

Despite many microorganisms utilizes nicotinic acid (NA) as sole N-source, only prokaryotic pathways were studied so far. Needless to say, eukaryotes, such as the model organism *Aspergillus nidulans* also has to have a set of enzymes and regulator(s), which makes the degradation of this compound possible. Beside the fact, that the revealing of the *A. nidulans* NA degradation (ND) pathway is expected to have an impact on basic sciences, its industrial usefulness is reasonably anticipated. As we expected, the eukaryotic pathway differs from the known prokaryotic routes, therefore the pathway enzymes most probably bear novel properties that can be potentially used in bioconversion processes to produce precursors of agro-industrially and therapeutically useful compounds. In this project we completely revealed the genetic background of one ND cluster (NDC1), composed of two transporter genes (*hxnP, hxnZ*), three enzyme coding genes (*hxnS, hxnT, hxnY*), and the transcription factor gene (*hxnR*) of the whole NA utilization pathway. On the basis of transcriptome analysis of our dually localized chromatin associated HmbB deletion mutant, we successfully predicted the existence of a second (NDC2) and a third cluster (NDC3). Comparative *in silico* analysis of the presence of the NDC1 genes among fungi along with the identification of *hxn6* allele (doesn't utilize NA and its 6-hydroxy derivative (6-NA)) by *A. nidulans* GeneBank transformation experiment predicted the existence of NDC2. We deleted all members of the NDC1 cluster. Generated mutants were further analysed. Identification of gain-of-function (constitutive) and loss-of-function mutations of the Cys2H2 Zn finger transcription factor HxnR along with *in silico* modeling revealed the structural and functional properties of HxnR.The astonishing resemblance of the amino-terminal part of HxnR to importin-3 makes this structural feature unprecedented. We proved that the NDC1 gene *hxnS* codes for the molybdenum cofactor (MOCO) protein PHII (purine hydroxylase II), which use both hypoxanthine and NA as substrate (prokaryotic MOCO xanthine dehydrogenases (XDH) have only one substrate, namely NA). We studied the function-related structural differences between PHII and its paralogue PHI, the latter belonging to the purine degradation pathway. The *hxnS* deletion mutant doesn't utilize NA and hypoxanthine as sole N-source and grows on 6-NA. This confirms that the first step of NA degradation in *A. nidulans* involves a molybdenoprotein XDH similarly to prokaryotes and the produced metabolite is 6-NA. Study of the expression of *hxnS* and *hxnP* revealed several conclusions: i.) the true metabolic inducer of the NA pathway is downstream from NA, ii.) the ammonium is a strong metabolic repressor and iii.) beside the pathway-specific transcription factor HxnR, AreA (a general co-regulator of N-metabolit pathways) acts as a co-regulator. HxnP and HxnZ are transporters, which of them HxnP seems to be a carrier of 6-NA. Intriguingly both *hxnT* and *hxnY* deletion mutants utilizes NA as sole N-source but show reduced growth on 6-NA. The growth reduction is additive in the *hxnT/hxnY* double mutant, which suggest two assumptions: i.) there must be an alternative route between NA and the metabolite downstream from 6-NA, and ii.) the HxnT and HxnY are on the same branch of the splitted pathway. We propose an

alternative product for HxnS, which is converted further either by HxnS itself or by a yet-unknown enzyme. We also located NDC2 cluster, composed of 3 enzyme coding genes. The expressions of the NDC1 genes are regulated by the NA pathway specific transcription factor and metabolite. The deletion mutants of NDC2 genes are under preparation and the preliminary results indicate that NDC2 products are pathway enzymes downstream to HxnS/hxnT/hxnY. Additionally a third cluster (NDC3) composing of two enzyme coding genes was predicted to have role in the ND pathway. This assumption is based on the fact, that the chromatin associated structural HmbB protein modulates the members of the NDC3 cluster and the NDC1 - NDC2 genes alike.

This ongoing research was continuously presented on international and national conferences, with 10 presentations (9 posters and 1 lecture). Preparation of a manuscript based on the results on the analysis of the NDC1 cluster is already in progress. The results and figures shown in this report outline the high quality of this study, which is anticipated to be released in a top rank journal with high impact factor, and is expected to be a highly cited reference for future studies.

Content:

1. Brief Introduction

Two molybdenum-containing enzymes of the xanthine dehydrogenase (XDH) family have been described in *Aspergillus nidulans*. One, called purine hydroxylase I (PHI) is a typical xanthine dehydrogenase (Glatigny & Scazzocchio, 1995; Lewis *et al.*, 1978; Mehra & Coughlan, 1989). The second enzyme, called purine hydroxylase II (PHII) has unprecedented substrate specificity. It accepts hypoxanthine and some other purines, but not xanthine as a substrate. It is competitively rather than irreversibly inhibited by allopurinol. Most remarkably it accepts nicotinic acid as a substrate (Coughlan *et al.*, 1984; Lewis *et al.*, 1978; Mehra & Coughlan, 1989; Scazzocchio, 1973) and it catalyses the first step of nicotinic acid catabolism (see below).

After PHII was first identified (Lewis *et al.*, 1978; Scazzocchio *et al.*, 1973), a number of bacterial NA hydroxylases, XDH-like enzymes were described, but to our knowledge, it has not been reported that any of the bacterial nicotinate hydroxylases could also accept purines as substrates.

PHII is completely absent in mycelia grown in neutral nitrogen sources (such as urea, acetamide or nitrate), it is induced by nicotinic acid but it is also present in nitrogen-starved mycelia (Scazzocchio, 1973)(the latter confirmed recently by RNAseq). The actual inducer of PHII is not nicotinic acid itself, while 6-hydroxynicotinic acid, the putative product of nicotinic acid hydroxylation behaves as an inducer (Sealy-Lewis *et al.*, 1979). The expression of PHII is not under the control of UaY, which is a transcription factor specific for the expression of the genes in the purine utilization pathway (Cecchetto *et al.*, 2012; Galanopoulou *et al.*, 2014; Gournas *et al.*, 2011; Scazzocchio *et al.*, 1982; Suarez *et al.*, 1995).

Nicotinic acid induces PHII, which can catalyse the hydroxylation of hypoxanthine to xanthine. Xanthine is further hydroxylated to uric acid by an α-ketoglutarate dependent xanthine dioxygenase encoded by

the *xanA* gene (Cultrone *et al.*, 2005; Darlington & Scazzocchio, 1968; Lewis *et al.*, 1978; Montero-Moran *et al.*, 2007). The steps and enzymes involved are shown in Fig. 1. The induction pattern of PHII implies that the enzyme belongs physiologically to the nicotinate utilization pathway.
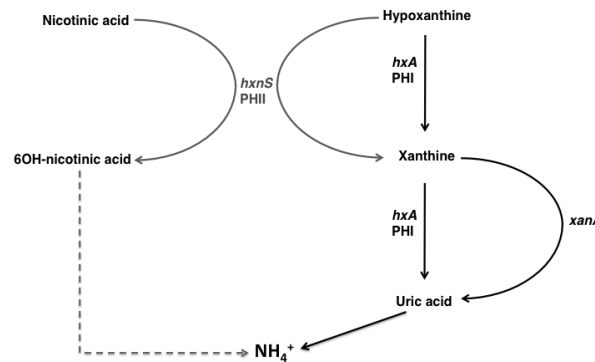
Fig. 1 The metabolic cross-talk between the purine and nicotinate utilization pathways.
PHI is a conventional xanthine dehydrogenase able to catalyse the conversion of hypoxanthine to xanthine and xanthine to uric acid. XanA is an α-ketoglutarate dependent xanthine dioxygeanase accepting xanthine but not hypoxanthine as a substrate. From there uric acid is converted to ammonium ($NH4^+$) by the well-established purine utilization pathway (Gournas *et al.*, 2011). PHII is an unconventional MOCO carrying enzyme hydroxylating hypoxanthine (but not xanthine) and nicotinic acid presumably to 6-hydroxy-nicotinic acid. As this latter compound is a nitrogen source it is presumably converted to ammonium, which is indicated by a dashed connector. In black: steps induced by uric acid, under the control of the UaY transcription factor. In grey: steps induced by nicotinic acid, 6-hydroxy nicotinic acid or a further metabolite in the nicotinate utilization pathway and actually (*hxnS*, PHII) or presumably under the control of the HxnR/AplA transcription factor(s). Full references are given in the text.

Mutants were isolated, which are able to grow on hypoxanthine as nitrogen source, but are unable to grow on media that contains hypoxanthine, allopurinol and nicotinic acid (1 mM).At this concentration, this compound does not serve as an efficient nitrogen source but fully induces PHII (described in Scazzocchio, 1973). The wild type grows on this medium, as PHII (resistant to allopurinol inhibition) (Lewis *et al.*, 1978; Scazzocchio *et al.*, 1973) hydroxylates hypoxanthine to xanthine which is further hydroxylated to uric acid by the XanA protein (Fig. 1). For this study, some of these mutants (*hxnS41, hxnS35, hxnS29, hxnR2* and *hxnR3*) were kindly provided by Prof. Scazzocchio (Imperial College, London, UK).

Constitutive mutants for PHII were selected on media that contains hypoxanthine and allopurinol (no nicotinic induction was supplied). Mutations were mapped in a gene they called *aplA* (Scazzocchio *et al.*, 1973). These mutations are dominant based on growth tests and they are semi-dominant at the level of enzyme assays. The authors interpreted these mutations as gain of function mutations (Scazzocchio, 1973). Few of these mutants were kindly provided by Prof. Scazzocchio.

The abovementioned studies clearly outlined the very first step of a eukaryotic nicotinic acid degradation pathway by the role of PHII and described closely linked pathway regulatory factors, HxnR and AplA[c]7. Using previous knowledge, summarized in Fig. 1, our main goal was to reveal the genetic background of the nicotinic acid utilization pathway. The results written here are not published yet, therefore we give a detailed account of our results here.

2. The NDC1 cluster

As a preliminary research of this OTKA project, the Principal Investigator of this project participated in a research at the University of South-Paris, France, where she complemented two different mutations with the same cosmid transformation: a nicotinic acid non-utilizer purine hydroxylase II (PHII) mutation *hxnS41* and a nicotinic acid/6-hydroxynicotinic acid non-utilizer mutation *hxnR2. The* cosmid W31H08 (from pLORIST2 based genomic library, obtained from the Fungal Genetic Stock Center, University of Missoury, Kansas City) carried the possible paralogue of the purine hydroxylase I (PHI) coding gene, *hxA*. The cosmid complemented both *hxnS41* and *hxnR2* loss-of-function mutations, indicating the close genetic linkage of *hxnS* and *hxnR.* Sequence analysis of the region

revealed the putative *hxnS* gene, which encodes a protein of 1396 residues, that is 33 residues longer than *hxA* coded PHI (1363 residues). The computed molecular weight of the HxnS monomer is 153,170.72, pI 5.91, compared to 149,523.49, pI 5.93 for HxA. These data are in accordance with the molecular weights experimentally determined for PHI and PHII native dimers (respectively 304.000 and 327.000, Lewis et al., 1978). We deleted the putative *hxnS* by Chaveroce's method (Chaveroche *et al.*, 2000). The method uses phage λ Red expressing *E. coli* strain (KS272) for obtaining the gene replacement by introducing a cosmid subclone carrying the candidate gene and a PCR product of a transformation marker gene (zeocin resistance gene) flanked with 50 bp regions of homology with the target DNA into the *E. coli* KS272 strain. The recombinant cosmid subclone obtained by *in vivo* recombination in *E. coli* KS272 carries the desired gene replacement and is used for *A. nidulans* transformation in order to obtain an allelic exchange between the mutant allele on the cosmid subclone and the wild-type locus. The obtained *hxnSΔ* strains served as a basisof this proposed project and together with the below detailed results are under publication.

2.1. Characteristics of HxnS comparing to other xanthine dehydrogenases

The *hxnSΔ* strain is able to grow on hypoxanthine, but unable to utilize nicotinate as a nitrogen source, unable to grow on media containing hypoxanthine, allopurinol and 1 mM nicotinic acid or hypoxanthine, allopurinol and 1 mM 6-hydroxynicotinic acid, but able to utilize 6-hydrocynicotinic acid, which phenocopies the previously isolated *hxnS* mutations (Fig. 2).
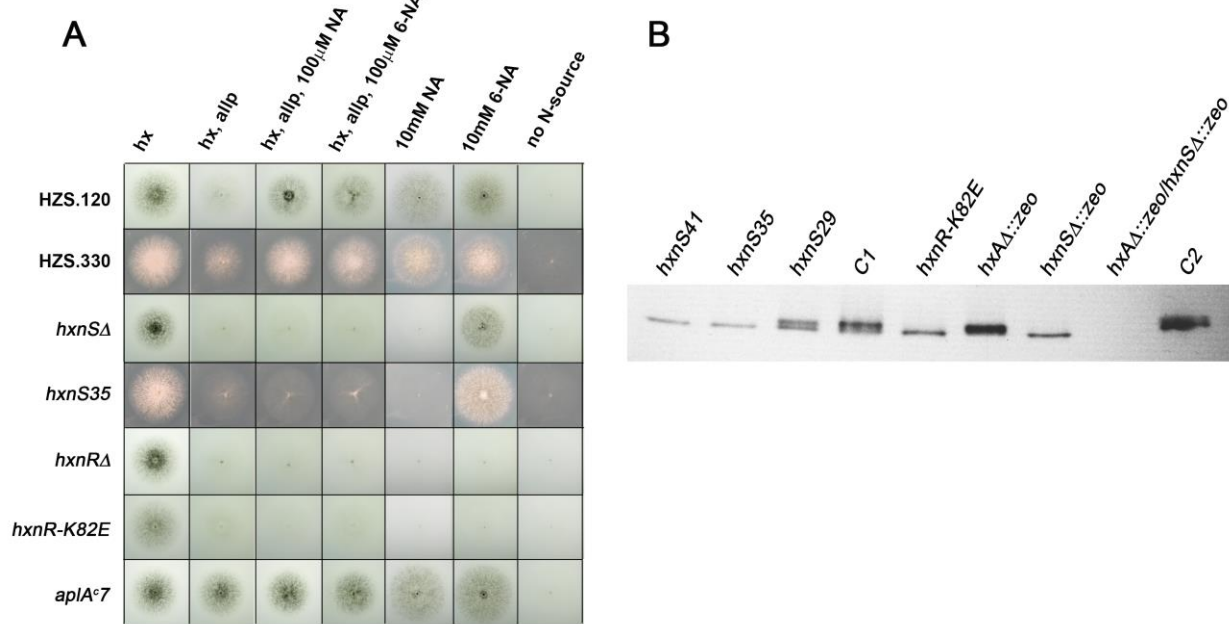
Figure 2. Presentation of the phenotype of *hxnS* and *hxnR* mutants by growth test and protein assay.
Panel A. Growth test of *hxnS* loss-of-function mutants and *hxnR* loss-of-function and gain-of-function mutants. hx: medium with hypoxanthine as N-source; hx, allp: hypoxanthine medium supplemented with allopurinol in order to inhibit PHI enzyme activity; hx, allp,100µM NA: hypoxanthine medium supplemented with allp and nicotinic acid (inducer of nicotinate utilization); hx, allp,100µM 6-NA: hypoxanthine medium supplemented with allp and 6-hydroxynicotinic acid (inducer of nicotinate utilization); 10 mM NA: medium with nicotinic acid as N-source; 10 mM 6-NA: medium with 6-hydroxynicotinic acid; no N-source: medium without N-source. HZS.120: control strain with green conidia (*riboB2 pabaA1 veA1*); HZS.330: control strain with white conidia (*wA3 pyroA4* actin-GFP(::pyrG::) (*pyrG89*)); *hxnSΔ*: *hxnS* deleted strain HZS.254 (*hxnSΔ::zeo biA1 veA1*); *hxnS35*: *hxnS* chain termination mutant HZS.110 (*hxnS35 aplAc7 biA1 wA3 veA1*); *hxnRΔ*: *hxnR* deleted strain HZS.136 (*hxnRΔ::zeo pantoB100 veA1*); *hxnR-K82E*: *hxnR* non-functional mutant HZS.220 (*hxnPΔ::riboB⁺ riboB2 hxnR-K82E pyroA4 nkuAΔ::argB⁺ veA1*); *aplAc7*: gain-of-function (constitutive) mutant of *hxnR* FGSC A872 (*aplAc7 biA1 veA1*). Growth plates with hypoxanthine N-source media were incubated for 2 days at 37°C and nicotinic acid or 6-hydroxynicotinic acid N-source media were incubated for 6 days at 37°C.
Panel B. Protein assay confirmation of the identity of HxnS and PHII described by Scazzocchio et al. (1973) . The missense mutation carrier *hxnR* mutant *hxnR-K82E* is also shown HZS.220 (*hxnPΔ::riboB⁺ riboB2 hxnR-K82E pyroA4 nkuAΔ::argB⁺ veA1*). *hxnS41* and *hxnS35*: chain termination alleles of *hxnS* in HZS.109 (*hxnS41 aplAc7 biA1 wA3 veA1*) and in HZS.110 (*hxnS35 aplAc7 biA1 wA3 veA1*); *hxnS29*: missense mutant allele resulting loss-of-function in HZS.113 (*hxnS29 pyrG89 pantoB100 biA1 veA1*);

hxnR-K82E: missense mutation allele of *hxnR* resulting loss-of-function in HZS.220 (*hxnPΔ::riboB⁺ riboB2 hxnR-K82E pyroA4 nkuAΔ::argB⁺ veA1*); *hxAΔ*::zeo: hxA deleted strain HZS.245 (*hxAΔ::zeo riboB2 pantoB100 biA1 veA1*); *hxnSΔ::zeo*: hxnS deleted strain HZS.250 (*hxnSΔ::zeo biA1 veA1*); *hxAΔ::zeo/hxnSΔ::zeo*: double-deleted *hxA/hxnS* mutant HZS.106 (*hxAΔ::zeo hxnSΔ::zeo pyrG89 pantoB100 biA1 pyr4 in trans*); C1: *hxA⁺ hxnS⁺* control strain HZS.185 (*riboB2 pyroA4 nkuAΔ::argB⁺ veA1*); C2: *hxA⁺ hxnS⁺* control strain HZS.145 (*veA1*). Strains were grown in acetamide media for 15 h at 37°C and then 1 mM 6-hydroxynicotinic acid was added to the media and further incubated for 5 h. Native PAGE of crude protein extracts were stained with hypoxanthine-tetrazolium.

A comparison of PHI (HxA) and PHII (HxnS) is shown in Fig. 3. We have sequenced the mutational changes in three extant *hxnS* mutations. *hxnS35* is a five base pair deletion between DNA positions 182 and 185 after the ATG, resulting in stop codon at residue 98, *hxnS41* is a double mutant (G3064T plus a deletion of 3066) resulting in a chain termination at residue 1162, while *hxnS29* (T3668C) results in a F1213S change in a conserved region 5, Fig. 3, Table I.). *hxnS35* and *hxnS41* result in loss of PHII as assessed by growth tests on hypoxanthine medium with allopurinol and 1 mM 6-hydroxynicotinic acid growth test and medium with 10 mM nicotinic acid as N-source (Fig. 2) and also by enzyme activity assay (Fig. 4). The *hxnS29,* a leaky mutation, shows no growth on nicotinic acid but grows on hypoxanthine medium with allopurinol and 1mM 6-hydroxynicotinic acid (Fig. 2) and shows a positive enzyme activity with hypoxanthine substrate. The sequence of these mutations is a formal evidence of the identity of the open reading frame of HxnS and PHII, encoded by the *hxnS* gene. The *hxnS* open reading frame is interrupted by three introns, none of which is the same position as those of interrupting the *hxA* open reading frame (Fig. 3).
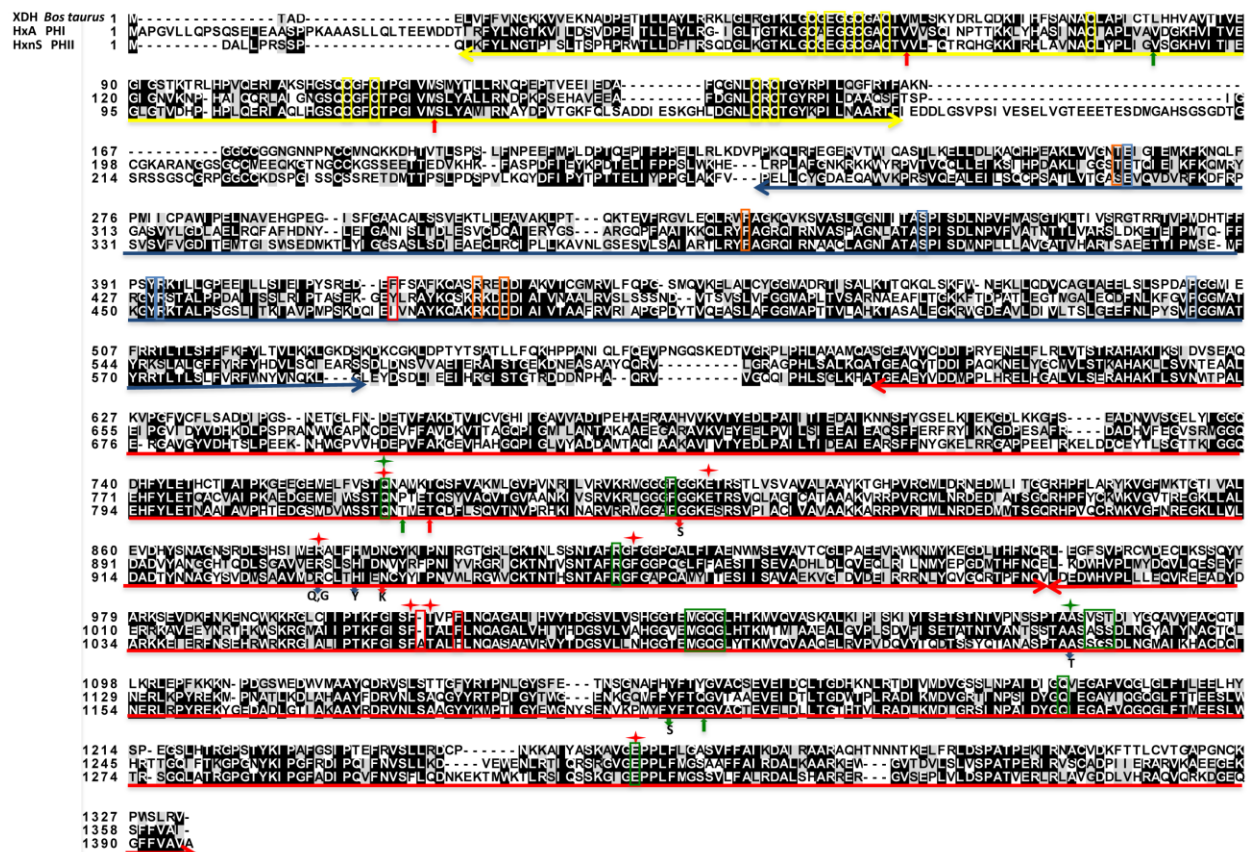
Figure 3. Comparison of PHI (HxA) and PHII (HxnS)
Sequence alignment of the two A. nidulans open reading frames is compared with the structurally characterised XDH from *B. taurus* (Enroth *et al.*, 2000). Underlying the sequences: Yellow, 2Fe2S clusters, blue FAD/NAD binding domain, red MOCO/substrate binding sub-domains I and II (Hille, 2005). Red arrows underlying the sequences indicate intron positions in the *hxA* gene, while green arrows indicate intron positions in *hxnS*. Boxed residues: Yellow, conserved Cys in the 2Fe2S clusters, also indicated E45 and G46 residues belonging to the Fe/S2 biding loop, and separating this cluster from the flavin ring; orange FAD binding residues (Enroth *et al.*, 2000); blue NAD+/NADH interacting residues (Ishikita *et al.*, 2012); Green, residues interacting with MOCO, red putatively functionally important residues where HxnS and its putatitve orthologues differ from both HxA and typical XDHs represented by the *B. taurus* and HxA sequences. Residues indicated by red crosses involved in substrate binding. Red downward arrows indicate mutational changes leading to complete loss of function in HxA, blue downward arrows indicate mutations leading to changes of substrate and inhibitor specificity in HxA (Glatigny & Scazzocchio,

1995), the downward green arrow indicated the only missense extant mutation sequenced for HxnS (see Table I.). Alignment with MAFFT E-INS-i, visualized with BoxShade.

The drastic differences in substrate and inhibitor specificities between PHI and PHII (described by (Coughlan *et al.*, 1984; Lewis *et al.*, 1978; Scazzocchio, 1973), are not obviously reflected in the sequence differences seen between HxA and HxnS. The residues involved in the two amino terminal 2Fe/2S clusters, the FAD and NAD binding residues, identified in the crystal structure of the *Bos taurus* enzyme are strictly conserved. Comparative analysis of HxnS and its putative fungal orthologues revealed the conserved features of HxnS. HxnS comprises several insertions when compared with HxA and characterized XDHs. The first insertion occurs between the second and the third Cys residues of the second 2Fe2S cluster. The sequence connecting the 2Fe/2S cluster domain and the FAD/NAD binding domain is considerably longer in HxnS, while the length of this sequence in HxA is similar to that of the *B. taurus* XDH. Within the FAD/NAD domain, the residue corresponding to 417(F) of the *B. tauru*s XDH is almost universally an aromatic residue in XDHs (Y454 in HxA) but it is Ile (I478) in HxnS and always an aliphatic hydrophobic residue in HxnS putative orthologues. The carboxy-terminus MOCO/substrate binding domain (from residue 590 in the *B. taurus* XDH) shows complete conservation of both the residues interacting with MOCO and with substrates (Arg 880 of *B. taurus* XDH, Arg 911 of HxA and Arg 935 of HxnS). Mutations affecting this residue in *hxA* (R911Q and R911G) result in altered substrate specificity including a PHII-like resistance to allopurinol inhibition and inability to accept xanthine as a substrate (Glatigny & Scazzocchio, 1995; Sealy-Lewis *et al.*, 1978). E803 of the *B. taurus* enzyme is also strictly conserved in HxA (E832) and HxnS (E855). This residue is never conserved in aldehyde oxidases (Garattini *et al.*, 2008). Mutations in the corresponding human XDH sequences (R881M and E803V) are individually sufficient to shift the substrate specificity of the human XDH to that of an aldehyde oxidase (Yamaguchi *et al.*, 2007). A number of residues within the HxA MOCO/substrate binding domain have been mutated to either missense loss-of-function or altered specificity phenotypes (Glatigny & Scazzocchio, 1995). All these residues are conserved in HxnS. A striking exception to the sequence conservation is the insertion of an Ala (A1067 in HxnS) between the almost universally conserved (in characterized or putative XDHs, but not always in aldehyde oxidases) (Garattini *et al.*, 2008) Phe1009 and Thr 1010 (numeration as in the *B. taurus* enzyme, corresponding to F1040 and T1041 in HxA, F1066 and T1068 in HxnS). This Phe/Thr pair is also conserved in bacterial XDHx (residues 459 and 460 in sub-unit B of the *Rhodobacter capsulatus* XDH) (Truglio *et al.*, 2002).
The absolutely conservation of this insertion in fungal HxnS orthologs will be discussed in the following section. Phen1013 is universally conserved in XDHs (F1044 in HxA), but it is a His (H1069) in HxnS and its putative orthologues. Not surprisingly both HxA and HxnS can be modelled and superimposed to the structure of the *B. taurus* XDH.

2.2. Phylogeny of *hxnS*

We proposed that *hxnS* originated from a gene duplication of an ancestral *hxA*-like gene (Lewis *et al.*, 1978). The availability of whole genome sequences of hundreds of fungi allows us to pinpoint the occurrence of this duplication. No *hxnS*-like gene is present in members of the Saccharomycotina, Taphrynomycotina, Basidiomycotina (but see below) or in any of the non-dicarya. The appearance of an *hxnS*-like gene coincides with the origin of the Pezizomycotina. Fig. 4 shows a simplified phylogeny, including only representative species. Duplicated *hxA*/*hxnS* genes are present in the basal class Pezizomycetes (such as *Tuber melanosporum*) but *hxnS* orthologues are absent from the two species of Orbiliomycetes where genome sequences are available. With one exception, to be discussed in Supplementary data, all species where a putative orthologue of HxnS is present, also carry an orthologue of HxA. Many episodes of loss of *hxnS* orthologues have occurred. Within the Eurotiomycetes, orthologues of HxA are present in all species available, but the presence of HxnS is patchy, present in the *nidulantes* group and the black Aspergilli, but not in *A. flavus,* it is only present in two species of *Penicillium* (*P. citrinum* and *P. paxilli).* Note however, that these two HxnS putative orthologues have an anomalous position in the tree clustering with the Sordariomycetales (Fig. 4).

Within the Sordariomycetales, a similar pattern occurs, with *hxnS* orthologues present in the *Fusaria*, but not in the Sordariales (such as *Neurospora crassa*, *Sordaria macrospora* and *Podospora anserina*).

We have noted in the previous section that the intron positions are different in *hxA* and *hxnS*. We could state that in no case throughout the available species these paralogues have introns in the same positions.
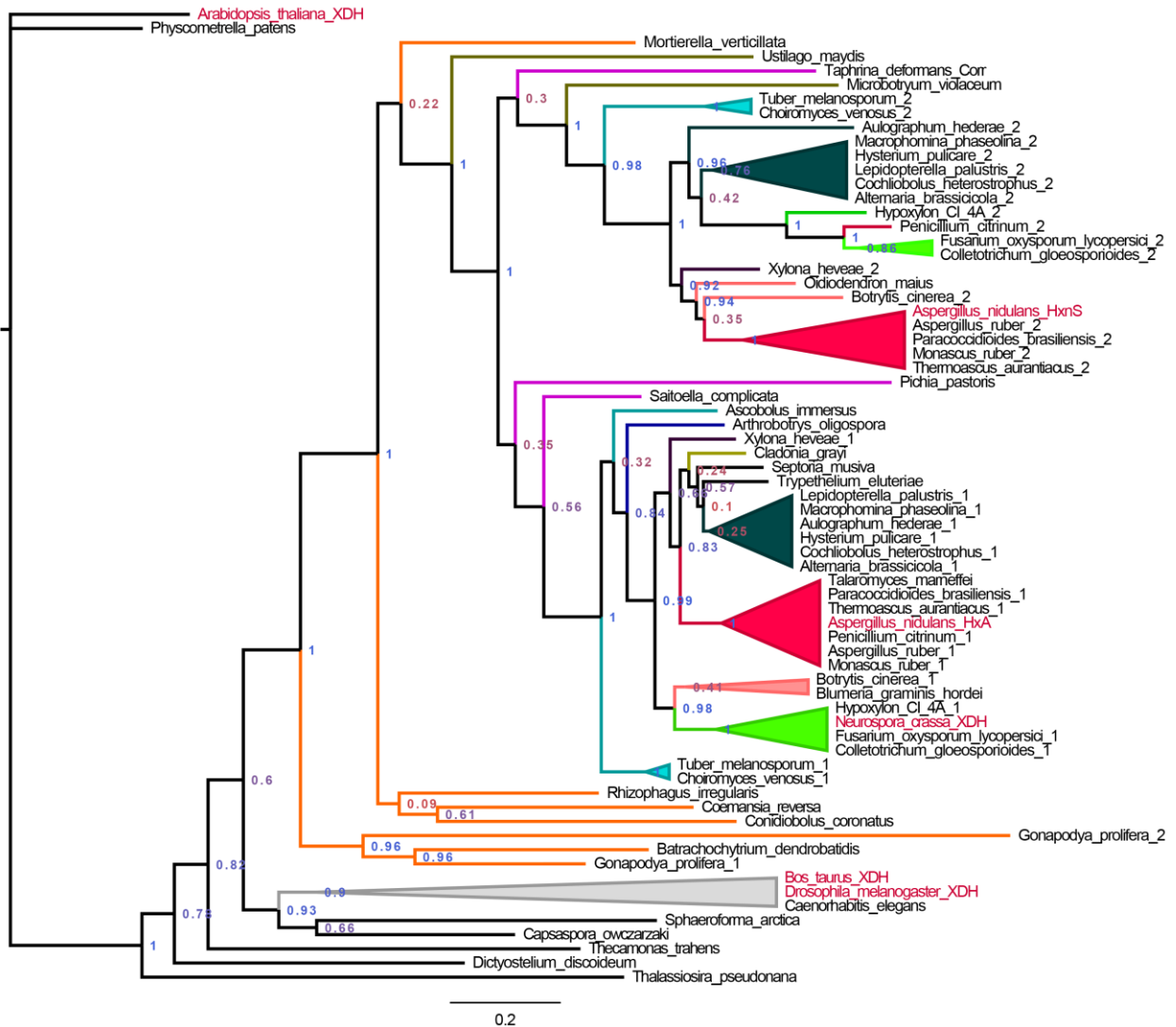
Figure 4. A maximum likelihood phylogenetic tree of fungal HxA (PHI) and HxnS (PHII) together with known or putative purine hydroxylases from other representative clades, included as out groups. Colour code, outgroups: Black viridiplantae (*Arabidopsis thaliana* and *Physcometrella patents*), Chromoalveolata, (*Thalassiosira pseudonana*), Amebeozoa *(Dictyostelium discoideum*), Apusozoa (*Thecamena trahens*), Filasterea (*Capsaspora owczarzaki*), Ichthyosporea (*Sphaerophorma artica*), grey animalia. Orange, non di-dicaryotic fungi, purple Taphrinomycotyna and Saccharomycotina, olive-green Basidiomycotina. Among the Pezizomycotina the following colour code was employed: Pezizomycetes, light blue; Orbiliomycetes, dark blue, Eurotiomycetes, red, Lecanoromycetes, very light blue; Dothideomycetes, dark green; Xylonomycetes, brown; Letiomycetes, yellow; Sordariomycetes, pale green. Red lettering indicates species where biochemical work on the cognate enzyme has been published. A red arrow indicates the notional duplication node where HxnS orthologues originated. Alignment carried out with MFFT E-INS-i, scoring matrix Blosum 62, alignment trimming with BMGE, Blosum 62, tree calculated with PhyML with automatic best model selection (LG) and rendered with FigTree. Values at nodes are aLRTs (approximate likelihood ratio test). Accession numbers are not shown here.

Two features of the tree deserve special mention. The genes of the two basal members of the Taphrynomycotina, *Saitoella complicata* and plant pathogen *Taphryna deformans* (Cisse *et al.*, 2013) are not clustered as would be expected. The former maps as an out group of the *hxA*-like genes of the Pezizomycotina, while the second appears as an outgroup of the *hxnS*-like genes Note that XDH-like proteins are absent from all species of *Schizosaccharomyces*, also members of the Taphrynomycotina,

8

which rely on XanA-like proteins for the first steps of purine utilization (Xanthine α-ketoglutarate dependent dioxygenase) (Cultrone *et al.*, 2005). The enzyme of *T. deformans* lacks the insertions interrupting the second 2Fe2S cluster and the one separating the latter from the FAD/NAD domain. I has a Phe residue at the position corresponding to 417(F) of *Bos taurus*, Y(454) of HxA and I487 of HxnS (see previous section and Fig. 3), however it carries a His at the position corresponding to in HxA (F1044) and HxnS (H1069). Finally, for the sequence FTL (1040-1041) of HxA and FATAL (1066-1069) of HxnS, we have FGAL (1032-1035) in the *T. deformans* enzyme. No biochemical work is extant in this species, nor it has it been reported whether it can utilize purines as nitrogen sources. Both *T. deformans* and *S. complicata* have the repertoire of genes encoding the enzymes of purine catabolism. The *T. deformans* genome does not have any of the genes to be reported below involved in nicotinate catabolism. It is thus possible that in spite of its phylogenetic position the *T. deformans* enzyme is a genuine XDH. Alternatively, it could be catalysing the hydroxylation of other hitherto unknown substrates. Its anomalous phylogentic position is most likely due to convergent evolution with the *hxnS*-like genes of the Pezizomycotina.

The second anomalous protein is that of the *Oidiodendron maius* (Letiomycetes, Heliotiales). The cognate protein maps within the Pezizomycotina *hxnS*-like clade. It shows both insertions in the 2Fe-2S cluster and between the 2Fe-2S domain and the FAD/NAD binding domain. It carries a hydrophobic residue (V534) where we have Y454 and I478 in HxA and HxnS respectively. It has a His (H1124) where HxA has F1044 and HxnS has H1069. However, it has FGAL (1120-1123) rather than FTAL (HxA1040-1042) or FATAL (HxnS1066-1070). Note that his sequence change is identical to that seen above for *T. deformans.* This putative HxnS orthologue is the only one among the Pezizomycotina which does not show the FATAL sequence.
Finally, the genomic sequence of the putative XDH ORF of *O. maius* is interupted by four introns. The first intron is in the same position of intron 1 of *hxnS* (Fig. 3), while other introns do not correspond to any of those extant in *hxA* or *hxnS*. We would propose that this enzyme is not a nicotinate hydroxylase but a classical XDH. *O. maius* has all the enzymes of purine breakdown, it even has an orthologue of UaY, the pathway specific regulatory gene characterized in *A. nidulans* and *N. crassa*. It has none of the nicotinate gene cluster genes to be discussed below. There is no other *hxA*/*hxnS* paralogue present in the genome. Thus is could be proposed that the orthologue of *hxA* was lost in this species, while the orthologue of *hxnS* mutated further to re-acquire an HxA like activity. Note however that *O. maius* has a perfect XanA orthologue, which could carry on its own the hydroxylation of xanthine.

2.3. Identification and characterisation of the *hxnR/aplA* gene coding for the pathway-specific transcription factor

Sequence analysis of genomic region upstream- and downstream to the *hxnS* gene revealed that closely linked to *hxnS*, but separated by an open reading frame of 998 nucleotides (to be called *hxnT*, see below) there is an open reading frame of 2673 nt encoding a protein of 865 residues comprising two typical Cys2H2 Zn fingers in its amino terminus. Between residues 394 and 668 a PFAM domain "Fungal transcription specific domain" PF04082 was detected. Strong predictions were obtained for both a monopartite NLS (VLRTRKMRRA) downstream from the Zn fingers by cNLS mapper, and an NES for residues 285-289 by NetNES.
We deleted the whole 2673 nt Cys2H2 Zn finger protein coding open reading frame. The resulting phenotype is identical to that reported previously for *hxnR* mutations (Scazzocchio, 1973; Scazzocchio, 1994) (see Fig. 2). We sequenced the whole open reading frame of strains carrying two *hxnR* (*hxnR2* and *hxnR3*) and two *aplAc* mutations (*aplAc7*, *aplAc48*) (extant mutants, gift from Prof. Scazzocchio). The results are shown in Table I. Both types of mutations map within the open reading frame of the 2673 nt Cys2H2 Zn finger protein. Thus we are dealing with one transcription factor gene that will be called *hxnR* rather than with two closely linked genes as previously proposed. The *aplA^c* mutations will be referred as *hxnR^c*. We attempted to define the domain of the *hxnR^c* mutations by selecting and sequencing additional constitutive mutations.

2.4. Developing and investigation of constitutive and loss-of-function *hxnR* mutations, modeling

For structure-function analysis, UV and 4-nitroquinoline 1-oxide (4-NQO) mutagenesis were applied on *hxAΔ* (HZS.248), *hxA18* (HZS.418) and *hxA⁺* (HZS.98) strains. *hxnR* constitutive mutants were selected on hypoxanthine medium supplemented with allopurinol. Strains able to grow on this medium were expectedly *hxnR* constitutive (*hxnR^c*) mutants. Application of alluporinol resulted in the complete inhibition of the PHI (HxA) in the recipient strain containing *hxA⁺* allele (HZS.98), therefore the hypoxanthine utilization must come from the PHII (HxnS), which needs the pathway inducer nicotinic acid or 6-hydroxynicotinic acid for the gene expression unless the pathway regulator *hxnR* transcription factor gaina mutation, that leads to constitutive expression. We assumed the occurrence of an alternative scenario in the *hxA⁺* allele containing HZS.98 or in the point mutation carrying *hxA18* strain HZS.418. Our assumption is that in the *hxA18* mutants the *hxA18* reverted back to wild-type allele, and then gained an allopurinol resistant mutation, which however resulted in a reduced growth on hypoxanthine in comparison to the *hxnR^c* mutants. According to the difference in the growth ability, the undesired *hxnR*-unrelated allopurinol resistant mutations can be distinguished from the *hxnR^c* mutations in a growth test. We selected 30 mutants and identified the constitutive mutations by sequencing their *hxnR* locus.

Table I. Gain-of-function and loss-of-function alleles of *hxnR* and *hxnS* identified by sequencing

hxnRc strains strains obtained by UV mutagenesis of HZS.248	**changed nucleotide**	**changed amino acid**
HZS.354	T751G	*hxnR^c-Y226D*
HZS.355	T757C	*hxnR^c-W228R*
HZS.452	C730G	*hxnR^c-P219A*
HZS.453	A1883C	*hxnR^c-K603T*
HZS.454	T751G	*hxnR^c-Y226D*
HZS.455	T751G	*hxnR^c-Y226D*
HZS.456	T751G	*hxnR^c-Y226D*
HZS.457	T751G	*hxnR^c-Y226D*
HZS.458	G1884T	*hxnR^c-K603N*
HZS.459	T751A	*hxnR^c-Y226N*
HZS.460	T757C	*hxnR^c-W228R*
hxnR^c strains strains obtained by 4-NQO mutagenesis of HZS.248		
HZS.461	G784T, G787C	*hxnR^c-D237Y,A238P*
HZS.462	G1884T	*hxnR^c-K603N*
HZS.463	T751A	*hxnR^c-Y226N*
hxnR^c strains strains obtained by UV mutagenesis of HZS.98		
HZS.464	T764C	*hxnR^c-F230S*
HZS.465	T757C	*hxnR^c-W228R*
HZS.466	T751G	*hxnR^c-Y226D*
HZS.467	A1882G	*hxnR^c-K603E*
hxnR^c strains strains obtained by UV mutagenesis of HZS.418		
HZS.468	C731T	*hxnR^c-P219L*
HZS.469	T757C	*hxnR^c-W228R*
HZS.470	T764C	*hxnR^c-F230S*
HZS.471	T757C	*hxnR^c-W228R*
HZS.472	A1894C	*hxnR^c-T607P*
HZS.473	T1769C	*hxnR^c-F565S*
HZS.474	A752C	*hxnR^c-A752C*

HZS.475	G758C	$hxnR^c$-W228S
HZS.476	T791C	$hxnR^c$-F239S
HZS.477	T1769C	$hxnR^c$-F565S
HZS.478	T763A	$hxnR^c$-F230I
HZS.479	A754G	$hxnR^c$-N227D

spontaneous $hxnR^c$ mutants obtained by selection on allopurinol from FGSCA26

$aplA^c$7	G1884T	$hxnR^c$-K603N
$aplA^c$48	C1990T	$hxnR^c$- R639C

$hxnR^-$ strains

hxnR2	G227A	hxnR-G76D
hxnR3	G1833A	hxnR-W578Opal
HZS.220	A244G	hxnR-K82E

As some mutational changes were detected several times, originating from different mutagenesis runs, we probably reached a near-saturation of constitutive mutations within the *hxnR* gene.

We detected putative HxnR orthologues only among the Pezizomycotina. As HxnR is the positive-acting transcription factor for *hxnS* and hitherto undetected (but see below) genes encoding downstream enzymes involved in nicotinate catabolism we would expect a strong correlation between the presence of a *hxnR* and *hxnS* orthologues. We constructed a CONSURF profile of the protein. This is shown in Fig. 5. It is satisfying that almost all miss-sense mutations, either constitutive or loss of function, mapped in highly conserved regions, most of them exposed. Constitutive mutations map in two patches, a well defined patch between residues 219 and 239, and in a wider domain between residues 565 and 639, located near to the carboxy terminal. For a number of residues we have obtained several different amino acid changes. We could propose that aromatic residues at position 226 and 228 and a basic residue at position 605 is necessary to maintain the protein in its physiological inactive state

Fig 5. The results of a CONSURF alignment of HxnR with 123 putative orthologues.
Alignment by MAFFT e-INS-i, loss of function mutation changes indicated in red, constitutive mutations indicated in green.

We conducted modeling of HxnR with I-Tasser, (http://zhanglab.ccmb.med.umich.edu/I-TASSER/ (Roy *et al.*, 2010; Zhang, 2008) and not surprisingly with high confidence it resulted in a perfect Cys2H2 Zn finger protein. The preliminary model is shown in Fig. 6. The ongoing marking of the Zn finger and placing of the Zn atom will make the model complete.
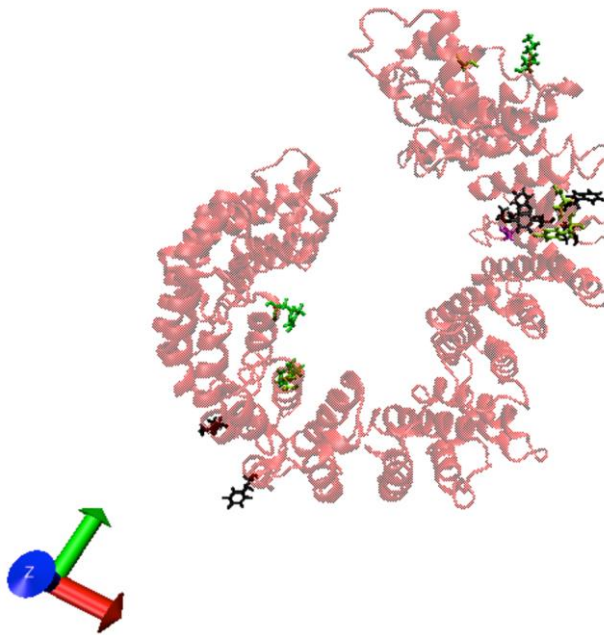
Figure 6. 3D model of HxnR
On the red helices of HxnR are shown the mutations presented in Fig. 5. Mutations at the top right are the two loss-of-function point mutations. The others are the constitutive mutations

Superimposition modeling brought a remarkably result. I-Tasser found a karyopherin, transportin-3, on which the N-terminal part of the Zn-finger domain folded in a perfect transportin-like structure. In Fig. 7 we show the superposition of the transportin-3 (in a complex with its ASF/SF2 molecules in the cavity) with the *HxnR*.
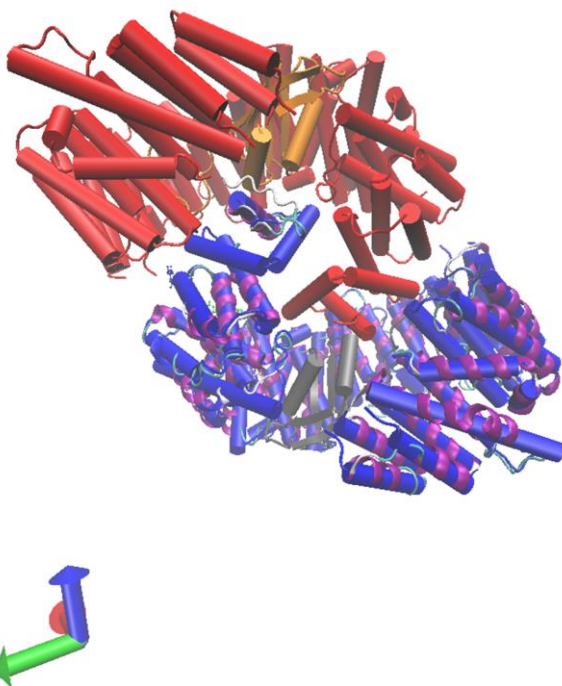
Figure 7. Model of hxnR (in purple helices) superimposed with a structure of two molecules of transportin-3.
Red and blue bundles of helices are two molecules of transportin-3. Purple helices show the model of HxnR. In the cavities there are (grey and orange) molecules of ASF/SF2, a small arginine serine rich splicing factor.

Validation of the model is under progress. The model, together with the detailed intracellular localization studies described below, proposed, that HxnR might show a nuclear membrane localization which is unprecedented among the transcription factors. The way we plan to shed light on the localization of HxnR in the future is detailed at the end of the *hxnR-gfp* localization analysis section.

13

All the obtained *hxnR^c* mutants were tested both in growth tests and protein assays. The *hxnR^c* mutants were able to grow on hypoxanthine medium supplemented with allopurinol while wild type did not (data not shown here). Hypoxanthine-tetrazolium based protein assay of *hxAΔ* and *hxA18* derived *hxnR^c* mutants showed the presence of HxnS activity when strains were grown up in the neutral acetamide N-source without having induction by either nicotinic acid or 6-hydroxynicotinic acid. The *hxA^+ hxnR^c* mutants, grown up in the neutral acetamide medium, were tested by nicotinate-tetrazolium protein assay in order to avoid the interference of HxA upon a hypoxanthine-tetrazolium assay. The wild type control does not showed enzyme activity in these assays. Fig. 8 shows a hypoxanthine-tetrazolium protein assay of the representatives of the various *hxnR^c* alleles.
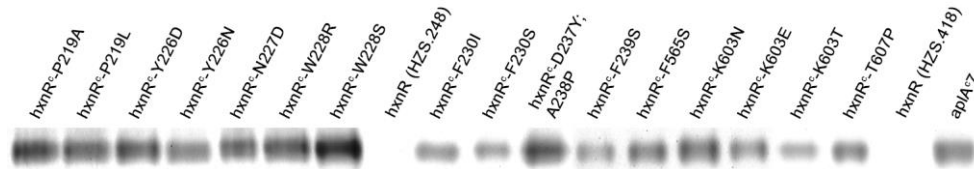
Figure 8.Hypoxanthine enzyme assay of selected *hxnR^c* allele-representatives of constitutive mutants.
hxnR^C-P219A: HZS.452 (*hxAΔ::zeo pantoB100 pabaA1 yA2 veA1 hxnRc-P219A*); hxnRc-P219L: HZS.468 (*hxA18 pantoB100 veA1 hxnR^C-P219L*); hxnR^C-Y226D HZS.354 (*hxAΔ::zeo pantoB100 pabaA1 yA2 veA1 hxnRc-Y226D*); hxnRc-Y226N: HZS.459 (*hxAΔ::zeo pantoB100 pabaA1 yA2 veA1 hxnR^C-Y226N*); hxnR^C-N227D: HZS.479 (*hxA18 pantoB100 veA1 hxnR^C-N227D*); hxnRc-W228R: HZS.355 (*hxAΔ::zeo pantoB100 pabaA1 yA2 veA1 hxnR^C-W228R*); hxnR^C-W228S: HZS.475 (*hxA18 pantoB100 veA1 hxnR^C-W228S*); hxnR (HZS.248): parental strain for mutagenesis HZS.248 (*hxAΔ::zeo pantoB100 pabaA1 yA2 veA1*); hxnR^C-F230I: HZS.478 (*hxA18 pantoB100 veA1 hxnR^C-F230I*); hxnR^C-F230S: HZS.464 (*pantoB100 pabaA1 veA1 hxnR^C-F230S*); hxnR^C-D237Y;A238P: HZS.461 (*hxAΔ::zeo pantoB100 pabaA1 yA2 veA1 hxnR^C-D237Y,A238P*); hxnR^C-F239S: HZS.476 (*hxA18 pantoB100 veA1 hxnR^C-F239S*); hxnR^C-F565S: HZS.473 (*hxA18 pantoB100 veA1 hxnR^C-F565S*); hxnR^C-K603N: HZS.458 (*hxAΔ::zeo pantoB100 pabaA1 yA2 veA1 hxnRc-K603N*); hxnR^C-K603E: HZS.467 (*pantoB100 pabaA1 veA1 hxnR^C-K603E*); hxnR^C-K603T: HZS.453 (*hxAΔ::zeo pantoB100 pabaA1 yA2 veA1 hxnR^C-K603T*); hxnRc-T607P: HZS.472 (*hxA18 pantoB100 veA1 hxnR^C-T607P*), hxnR (HZS.418): parental strain for mutagenesis HZS.418 (*hxA18 pantoB100 veA1*); aplA^C7: aplA^C7 control strain FGSC A872 (*aplA^C7, biA1, veA1*).

2.5. Study of intracellular localization of HxnR

We constructed three different *hxnR-gfp* fusion cassettes. Transcription of the cassette was under the control of 3 different promoters: the constitutive *gpdA*, the inducible *prnD* (induced by proline and repressed by ammonium), and the native *hxnR* promoter (induced by nicotinic acid or 6-hydroxynicotinic acid, repressed by ammonium) in the pAN-HZS-1 vector (Karacsony *et al.*, 2014). Prior to the cloning of the *hxnR*, the NcoI motif in the *hxnR* coding region was mutated by PCR based site directed mutagenesis using the Double-Joint PCR method (Yu *et al.*, 2004). The PCR product (*hxnR* without the stop codon and with a linker sequence of 9 AAs (LIDTVDLDS) was cloned into the NcoI site of the pAN-HZS-1 vector (Karacsony *et al.*, 2014). The developed vector pAN-HZS-7 expresses *hxnR-gfp* from the constitutive *gpdA* promoter and carries *pantoB^+* transformation marker (Fig. 9). From pAN-HZS-1 we developed a *prnD* promoter driven *gfp* expressing vector pAN-HZS-5 by cloning the 1572bp long promoter of *prnD* into the NheI-NcoI site of pAN-HZS-1 (Fig. 9). pAN-HZS-5 was used to construct the inducible *prnD* promoter driven *hxnR-gfp* vector pAN-HZS-6 by cloning the NcoI free *hxnR* to the NcoI site of pAN-HZS-5 (Fig. 9). The native *hxnR* promoter driven *hxnR-gfp* construction pAN-HZS-8 was made by cloning the *hxnR* promoter containing NcoI-site mutated 3006 bp long PCR product into the NcoI site of pAN-HZS-5 (Fig. 9). The *hxnR-gfp* cassettes in each developed vectors were sequenced prior to transformation. The construction work was presented as a poster on a Conference in 2015 (Poster abstract, Ámon et al. 2015)

14
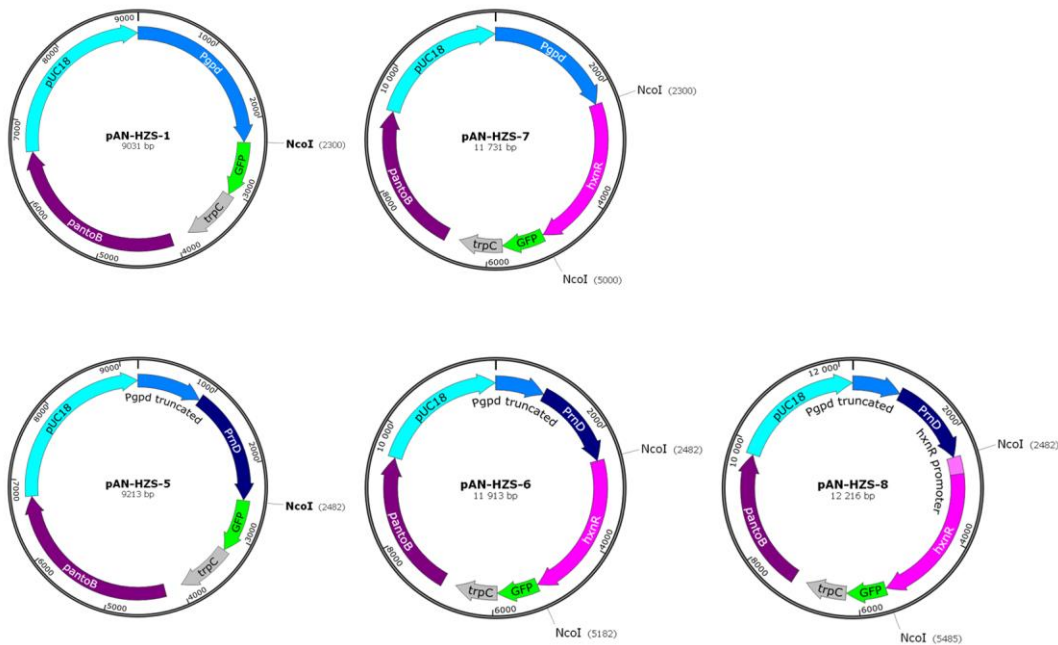
Figure 9. GFP expression vectors developed from pAN-HZS-1 (Karacsony et al. 2014).

A. nidulans hxnR∆ strain expressing red fluorescent protein labeled H1 histone (hhoA::mRFP) HZS.416 (*hxnR∆::zeo hhoA-mRFP-AfriboB⁺ pantoB100 (nkuA∆::argB⁺) veA1*) was transformed with *hxnR-gfp* expressing pAN-HZS-6, pAN-HZS-7 and pAN-HZS-8 vectors and the empty, *gfp* vectors pAN-HZS-1 (Karacsony *et al.*, 2014) and pAN-HZS-5 as controls. Transformants, prototrophic for pantothenic acid were selected. The fusions were integrated *in trans* of a *hxnR∆* mutation at random chromosomal loci in different copy numbers. The copy number of *hxnR-gfp* in the transformants was determined by qPCR using *hxnR* and *acnA* (gamma-actin) specific primer pairs using ∆∆Ct analysis. Selected transformants were tested in growth tests and used for fluorescence microscopy (Zeiss Axiolab A, Zeiss filter set 15 for GFP and Zeiss filter set 09 for mRFP). Samples for microscopic examinations were prepared by inoculation of 10^4 conidia onto coverslips dipped in medium and incubated at 37°C for 5-8 hours.

The constitutively expressed *gpdA* promoter driven *hxnR-gfp* carrying strains showed growth defects on minimal media (not shown here), as it is expected in case of the overexpression of a transcription factor (Kwon *et al.*, 2010; Wong *et al.*, 2009). Clear nuclear localization was detected under all tested conditions (data not shown). The *hxnR* promoter driven *hxnR-gfp* construction showed a partial and copy number dependent complementation of the *hxnR∆* phenotype (data not shown), however the GFP fluorescence signal was under the detection threshold, even in the transformant with the highest copy number *hxnR-gfp* (15 copies) (data not shown). The *prnD* promoter driven *hxnR-gfp* constructions complemented the *hxnR∆* phenotype in a similar way as can be seen in the *hxnR* promoter driven *hxnR-gfp* construction carrying transformants. The complementation was partial and copy number dependent under the experimental setup (Fig. 10).

The complementation of the *hxnR∆* phenotype by *prnD* promoter driven construction was tested on a medium where proline (which is a better N-source than nicotinic acid or hypoxanthine) was not added to the medium. Therefore the growth tests shown in Fig. 10 were performed under a non-induced condition in respect of the *prnD* promoter of the integrated *hxnR-gfp* constructions. The reason for we can see growth of some transformants is the leakiness of the *prnD* promoter. This leakiness afforded us to test the transformants for the complementation of the *hxnR∆* phenotype (strain 416 on Panel A, Fig. 10). On hypoxanthine medium supplemented with allopurinol and 1 mM 6-hydroxynicotinic acid, only the highest copy number transformant HZS.417 (trf/9 on Panel A, Fig. 10) was able to grow. The growth is very weak comparing to that of the *hxnR⁺* control HZS.145 (145 on Panel A, Fig. 10). When 1 mM nicotinic acid is used for induction (top right plate on Panel A, Fig. 10) the highest copy number transformant could not grow. We reasoned that the inducer of the nicotinic acid pathway is necessary for the pathway induction (PrnA and AlcR transcription factors behave similarly) (Nikolaev *et al.*, 2003;

15

Pokorska *et al.*, 2000) when HxnR is represented at a basal level (for basal level of *hxnR* expression on non-induced condition see the Northern result on Fig. 13). In the sections below, we show that the true inducer of the pathway is not the nicotinic acid, but a metabolite downstream to nicotinic acid (we revealed it by mRNA level studies, see the sections below, Panel B, Fig. 14). Therefore, HxnS must take part in the processing of the true inducer. Since HxnS shows a very poor kinetic parameters for nicotinic acid substrate (*Km* 189 µM in crude extract) (Coughlan *et al.*, 1984; Lewis *et al.*, 1978) and the availability of the enzyme product 6-hydroxynicotinic acid is limited for the downstream pathway enzymes for further processing. HxnS limits the availability of the true inducer and HxnR is not activated that is necessary for induction of the pathway. On a medium containing 10 mM 6-hydroxy nicotinic acid as a sole N-source (bottom right plate) only the transformants with 3 or higher copy number integration show growth (trf/1, trf/5 and trf/20 on Panel A, Fig. 10), while *hxnRΔ* control (416 on Fig. 10) did not grow. Using 10 mM nicotinic acid as sole N-source, the transformants show no growth, which can be explained with the abovementioned study about the low enzyme activity of HxnS on nicotinic acid substrate.

A
                                                   B
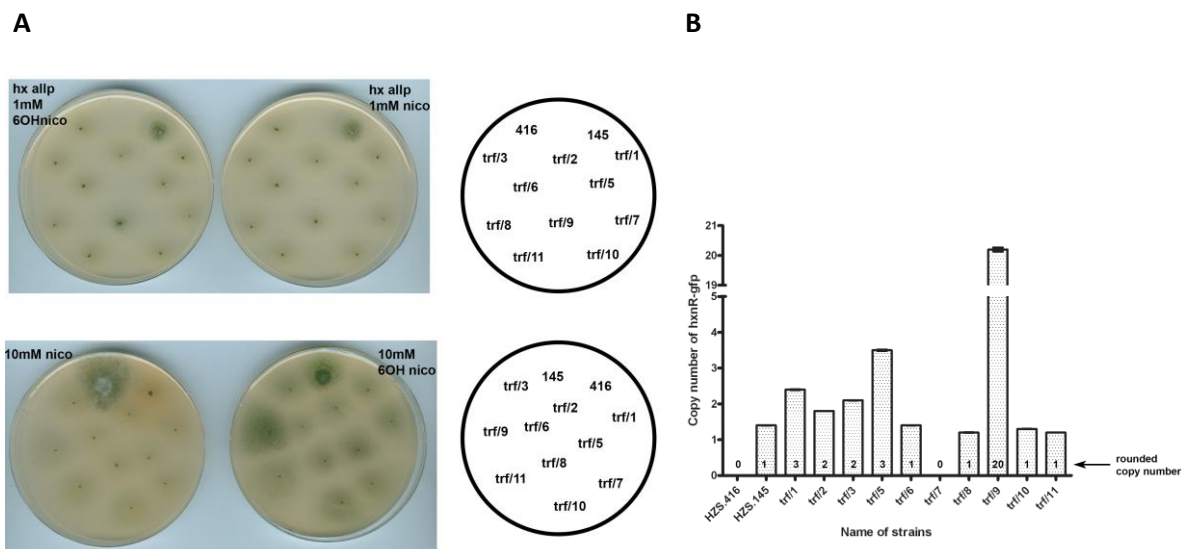
Figure 10. Growth of *prnD* promoter driven *hxnR-gfp* carrying strains and the copy number of the *hxnR-gfp* integrations *in trans*

Panel A. Complementation of the *hxnRΔ* phenotype by the *prnD* promoter driven *hxnR-gfp* carrying transformants on hx allp 1mM 6OHnico (hypoxanthine medium supplemented with allopurinol and 1 mM 6-hydroxynicotinic acid); hx allp 1mM nico (hypoxanthine medium supplemented with allopurinol and 1 mM nicotinic acid); 10 mM nico (medium with 10 mM nicotinic acid as N-source) and 10 mM 6OHnico (medium with 10 mM 6-hydroxynicotinic acid as N-source) media.

416: *hxnRΔ::zeo hhoA-mRFP-AfriboB⁺ pantoB100 (nkuAΔ::argB⁺) veA1* recipient strain (HZS.416) for transformation with pAN-HZS-5 and pAN-HZS-6 vectors; 145: control *veA1* strain (HZS.145); trf/1, 2, 3, 5, 6, 7, 8, 9, 10 and 11: transformants obtained by transformation of pAN-HZS-6 vector carrying *prnD* promoter driven *hxnR-gfp* into strain HZS.416; C4, C8 and C9: transformants obtained by the transformation of the empty pAN-HZS-5 vector into strain HZS.416 as a control. The schematic drawing of the plates next to the growth tests show the positioning of the tested strain.

Panel B. Copy number of *hxnR-gfp* integrations in the transformant and control strains.

Copy number was measured by qPCR using *hxnR* and *acnA* (gamma-actin) houskeeping gene specific primer pairs. Results were analysed by the ΔΔCt method. Standard deviations based on three replicates are shown.

Intracellular localization of HxnR under non-induced, induced and repressed condition was studied using the transformants with the hxnR-gfp construct under the control of the constitutive *gpdA* promoter, inducible *prnD* promoter and the native *hxnR* promoter. In case of the *gpdA* and the *hxnR* promoter constructions we used the neutral acetamide (1 mM) or urea (5 mM) as sole N-source for the first 4-5h of growth at 37°C, which was supplemented with 1 mM 6-hydroxynicotinic acid upon induction or 5 mM ammonium for repression and further incubated for 2h. In case of *prnD* promoter constructions we used medium with 5 mM urea as sole N-source and induced the promoter by the addition of 5 mM proline to the media for the last 2h of incubation. Induction by proline together with 6-hydrocynicotinic nicotinic acid was also tested. For the repression condition we had to circumvent the repression of *prnD* promoter caused by ammonium. Instead of glucose we used 2% proline as the sole

16

carbon source and at the same time it served as nitrogen source, too. When proline is utilized as a carbon source, the ammonium cannot repress the *prnD* promoter, therefore the effect of repressed condition on the HxnR localization can be studied.

HxnR localization in each of the *prnD* promoter driven *hxnR-gfp* transformants was monitored and qualitative difference in the HxnR-Gfp localization was not detected. For the study of the localization upon various growth condition we chose a transformant with 1 copy integration of *hxnR-gfp* (HZS.425: *hxnR∆::zeo hhoA-mRFP-AfriboB⁺ pantoB100 (nkuA∆::argB⁺) veA1* carrying ectopic pAN-HZS-6 plasmid in 1 copy) and a transformant with 20 copies integration (HZS.417: *hxnR∆::zeo hhoA-mRFP-AfriboB⁺ pantoB100 (nkuA∆::argB⁺) veA1* carrying ectopic pAN-HZS-6 plasmid in 20 copies).

The nuclear localization of HxnR was detected in each conditions tested (Fig. 11), similarly to AlcR (Nikolaev *et al.*, 2003) or PrnA (Pokorska *et al.*, 2000) transcription factors. Copy number differences did not affect the localization of *hxnR-gfp*, although the intensity of the GFP signal was slightly weaker in the HZS.425 strain (with 1 integration), in comparison with the HZS.417 strain (with 20 copies), according to our expectations.
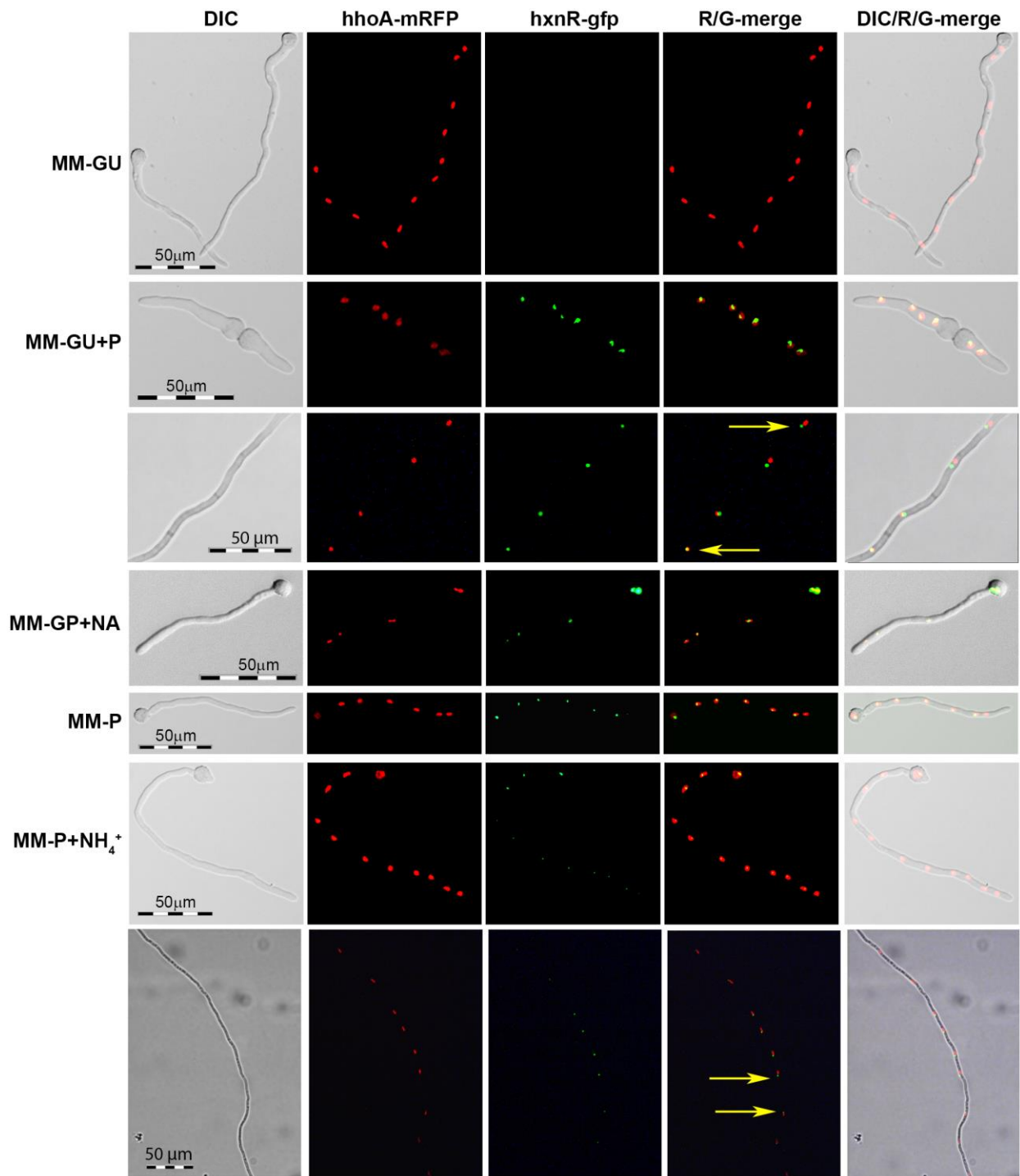
Figure 11. Nuclear localization of HxnR-Gfp in strain HZS.416 (*hxnRΔ::zeo hhoA-mRFP-AfriboB⁺ pantoB100 (nkuAΔ::argB⁺) veA1*) transformed with pAN-HZS-6 vector (PrnD promoter driven hxnR-gfp expression vector in 20 copy number).
DIC: DIC microscopy; hhoA-mRFP: fluorescence microscopy of HhoA-mRFP (red fluorescent protein fused to H1 histone); hxnR-gfp: fluorescence microscopy of HxnR-Gfp (green fluorescent protein fused to HxnR); R/G-merge: merged RFP and GFP signals; DIC/R/G-merge: DIC merged with the RFP and GFP signals. Zeiss 09 and 15 filter sets were used for mRFP and GFP, respectively. Scale bars represent 50 μm.

10^4 conidia were inoculated in duplicate onto coverslips dipped in MM-GU (minimal media with glucose as C-source and urea as N-source), MM-GP (minimal media with glucose as C-source and proline as N-source), in MM-P (minimal media with proline as C- and N-source) and incubated at 37°C for 3–5 h. One set of the cultures was treated with proline (5 mM), nicotinic acid (1 mM) and ammonium-d-tartrate (5 mM), which were supplemeted to the MM-GU, MM-GP and MM-P cultures, respectively (MM-GU+P, MM-GP+NA and MM-P+NH4+) while the other set of the cultures was left untreated. After additional 2 h of incubation at 37°C the young germlings on the coverslips were fixed by using 4% formaldehyde (in PBS pH7.5) for 45 minutes, and then the samples were monitored in fluorescent microscopy.

In some cases, the H1 histone fused mRFP fluorescence did not show colocalization with the HxnR-

fused Gfp fluorescence within the nuclei. We considered the probability of field-shifting in the microscope between two snapshots, however in some of the nuclei, the relative positioning of the green/red signal pairs (yellow arrow pairs on Fig. 11) clearly ruled out the possibility, that the separate localization of HxnR-Gfp and H1-mRFP is an artefact. We reasoned that the HxnR transcription factor localizes to the nuclear membrane. Considering the 3D model of HxnR superpositioning with exportin-3, together with the indicated sublocalization of HxnR makes reasonable to investigate the sublocalization of HxnR by Z-stacking confocal microscopy and Western blot analysis. Confocal microscopy might prove that co-localization of HxnR-Gfp signal with H1-mRFP signal is due to the accidental orientation of the red-labeled chromatin and the nuclear membrane-bound HxnR, hence fluorescence signals might originated from distinct compartments. Nuclear membrane localization of a transcription factor is unprecedented and would raise many questions about the the transcription activating role of this transcription factor. Western blot analysis carried out on *hxnR* promoter driven *hxnR-gfp* transformants (in 1 and 15 copies), *prnD* promoter driven *hxnR-gfp* transformants (in 1 and 20 copies) and Gfp expressing pAN-HZS-1 or pAN-HZS-5 transformants as controls under non-induced, induced and repressed conditions with Gfp antibody may reveal whether HxnR splits into two parts and move into the nucleus upon a certain condition. It may be possible that HxnR interacts with other proteins and exerts its function through that interaction. Considering that all the constitutive and loss-of-function mutations mapped to the outer surface of the protein (Fig. 6) makes this hypothesis worth to investigate.

2.6. Identification of NDC1 cluster genes, obtaining of deletion mutants

By scouting the close genomic linkage of *hxnR* and *hxnS*, we reasoned that similarly to prokaryotic nicotinic acid degradation pathway genes (Jimenez *et al.*, 2008), the *A. nidulans* pathway genes should also show clusterization. In order to test the hypothesis we systematically investigated the expression profile of the *hxnR* neighbouring genes by Northern analysis, which led us to the identification of a cluster (NDC1) of 6 genes (including *hxnS* and *hxnR*) (Fig. 12), which are induced by nicotinic acid, repressed by ammonium and requires the HxnR transcription factor for their expression (Fig. 13).
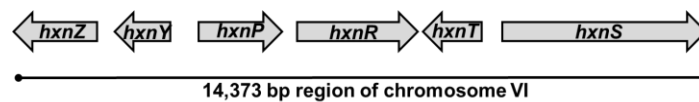
Figure 12. Arrangement of the nicotinic acid degradation cluster 1 (NDC1) on chromosome VI.
Arrows indicate orientation.

	hxnR2			wt			aplAᶜ7		
	N	I	R	N	I	R	N	I	R
hxnS	4	5	5	49	100	5	182	222	5
hxnR	21	21	8	80	100	8	106	147	17
hxnT	2	2	2	15	100	3	395	498	4
hxnZ	1	1	1	4	100	4	262	199	2
hxnY	2	2	1	47	100	2	288	151	0
hxnP	4	4	4	49	100	5	159	165	7
hxB	24	30	11	51	100	11	309	368	13
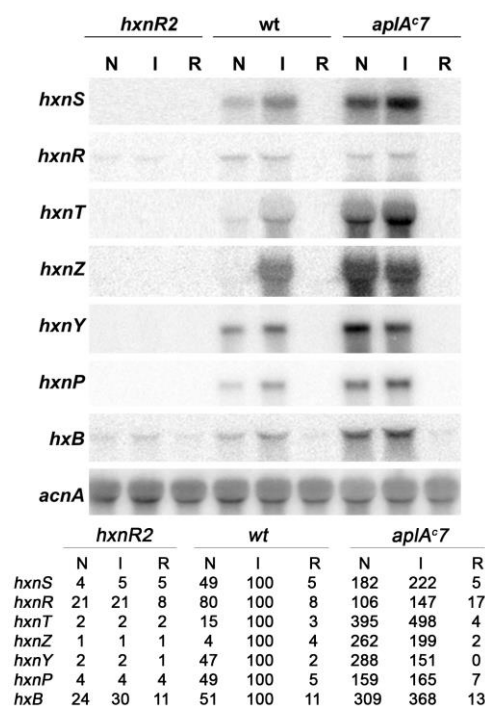
Figure 13. Northern analysis of NDC1 cluster genes (hxnS/R/T/Z/Y/P) and *hxB* in *hxnR2* loss-of-function mutant, *hxnR*[+] control strain and in *aplAc7* gain-of-function (constitutive *hxnR*) mutant under non-induced (N), induced (I) and repressed (R) conditions.
Strains were grown in MM media with acetamide as N-source for 8 hours at 37 °C then 1 mM nicotinic acid was added to the medium (I: induced condition), 5 mM ammonium-tartrate were added to the medium (R: repressed condition) or one set of culture medium was left untreated (N: non-induced condition). *acnA* codes for gamma-actin (housekeeping gene), *hxnS/hxnR/hxnT/hxnZ/hxnY* and *hxnP* are the NDC1 cluster genes, *hxB* encodes the enzyme responsible for the maturation of the MOCO cofactor, which is pivotal for HxnS (PHII) activity. The table below the Northern shows quantitative densitometry estimates of the *hxn* cluster gene and *hxB* mRNA steady-state levels expressed as percentage of the wild-type induced level.

NDC1 regulation is discussed in details in the sections below on the basis of qRT-PCR results processed by the standard curve method (Larionov *et al.*, 2005). The newly identified genes were called *hxnT*, *hxnY*, *hxnZ* and *hxnP*. The gene products are putative dioxygenases for HxnT and HxnY, while HxnP and HxnZ are transporters. Deletion of *hxnT/Y/Z/P* cluster genes were made as described previously (Karacsony *et al.*, 2014). The *hxnT/Y/Z/P* targeting substitution cassettes were constructed by the Double-Joint PCR method (Yu *et al.*, 2004), where the *riboB*[+] or the *pabaA*[+] genes were used as transformation markers. Deletions were carried out by transformation of the substitution cassettes into the *pabaA1 riboB2* or in the *riboB2 pyroA4* auxotrophic strains (HZS.120 and HZS.185, respectively). Transformants carrying single copy integration were selected for further experiments (see below). By genetic cross of *hxnTΔ* with *hxnYΔ* we obtained double deleted *hxnTΔ/hxnYΔ* strains. Growth test of mutants are (shown in Fig. 14)

2.7. Role of HxnY, HxnT, HxnP and HxnZ in the pathway

On 6-hydroxynicotinic acid *hxnTΔ* strain shows a reduced growth and *hxnYΔ* strain shows a very slight growth reduction. The growth reduction however is additive in the *hxnT/hxnY* double mutant, which verify that the subtle growth reduction seen in *hxnYΔ* is valid. 6-hydroxynicotinic acid is a substrate of HxnT and HxnY. Intriguingly the *hxnTΔ* and *hxnYΔ* strains do not utilize the upstream metabolite, nicotinic acid. The only possible reason of this phenomenon is that the nicotinate degradation pathway splits right after the nicotinic acid, which however predicts an unknown enzyme function of HxnS, besides the hydroxylation of nicotinic acid to 6-hydroxynicotinic acid.

20
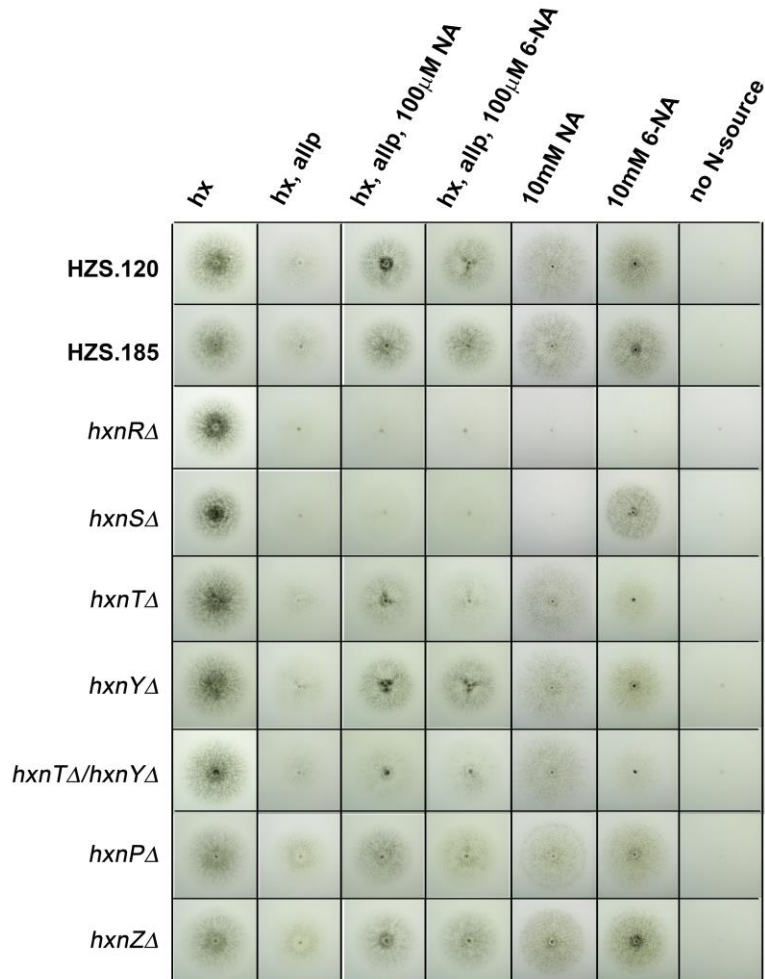
Figure 14. Growth test of nicotinic acid degradation cluster genes.
hx: medium with hypoxanthine as N-source; hx, allp: hypoxanthine medium supplemented with allopurinol in order to inhibit PHI enzyme activity; hx, allp,100µM NA: hypoxanthine medium supplemented with allp and nicotinic acid (inducer of nicotinate utilization); hx, allp,100µM 6-NA: hypoxanthine medium supplemented with allp and 6-hydroxynicotinic acid (inducer of nicotinate utilization); 10 mM NA: medium with nicotinic acid as N-source; 10 mM 6-NA: medium with 6-hydroxynicotinic acid; no N-source: medium without N-source. HZS.120: recipient strain for transformation to obtain *hxnTΔ* and *hxnYΔ* deletions (*riboB2 pabaA1 veA1*); HZS.185: recipient strain for transformation to obtain *hxnPΔ* and *hxnZΔ* deletions (*riboB2 pyroA4 nkuAΔ::argB⁺ veA1*); *hxnRΔ*: *hxnR* deleted mutant HZS.136 (*hxnRΔ::zeo pantoB100 veA1*); *hxnSΔ*: *hxnS* deleted strain HZS.254 (*hxnSΔ::zeo biA1 veA1*); *hxnTΔ*: *hxnT* deleted strain HZS.222 (*hxnTΔ::pabaA⁺ pabaA1 riboB2 veA1*); *hxnYΔ*: *hxnY* deleted strain HZS.223 (*hxnYΔ::riboB⁺ riboB2 pabaA1 veA1*);

hxnTΔ/hxnYΔ: *hxnT* and *hxnY* double deleted strain HZS.502 (*hxnTΔ::pabaA⁺ hxnYΔ::riboB⁺ riboB2 pabaA1 veA1*); *hxnPΔ*: *hxnP* deleted strain HZS.221 (*hxnPΔ::riboB⁺ riboB2 pyroA4 nkuAΔ::argB⁺ veA1*); *hxnZΔ*: *hxnZ* deleted strain HZS.226 (*hxnZΔ::riboB⁺ riboB2 pyroA4 nkuAΔ::argB⁺ veA1*). Growth plates with hypoxanthine N-source media were incubated for 2 days at 37°C and nicotinic acid or 6-hydroxynicotinic acid N-source media were incubated for 6 days at 37°C.

The alternative route between nicotinic acid and the 6-hydroxynicotinic acid downstream metabolite is unprecedented in prokaryotes and the hydroxylation of nicotinate to 6-hydroxynicotinic acid is a conserved common step in the degradation pathway (Alhapel *et al.*, 2006; Ensign & Rittenberg, 1964) processed by HxnS-like prokaryotic dehydrogenases. Processes downstream to 6-hydroxynicotinic acid may vary from prokaryote to prokaryote, however alternative routes were not described previously, in any of the species. This highlights that the utilization of nicotinic acid in *A. nidulans* operates differently from any known prokaryotes and the participating enzymes must bear with novel properties. Phenotype of *hxnTΔ* and *hxnYΔ* strains outlines the first steps of nicotinic acid degradation and suggests an alternative route, where an unknown hydroxylation product is produced by HxnS, which is further processed by either HxnS or by a yet undiscovered enzyme (Fig. 15). We tested the commercially available 2-hydroxynicotinic acid in growth tests as sole N-source (10 mM) or inducer (1 mM) in hypoxanthine allopurinol media and found that this compound could not be utilized by *A. nidulans*. Another potential alternative product of HxnS might be 5-hydroxynicotinic acid, which will be tested in the near future. We tested 2,5-dihydroxypyridine acid as sole N-source (10 mM) or inducer (1 mM) in hypoxanthine allopurinol media in growth tests but the results were not clear to assess the role of this compound in the pathway, yet to this point. Optimization of the solvent and the concentration of the stock solution is in the pipeline, and repetition of the growth test is under progress.

Parallel with the microbiological studies, we started to develop analytical methods to support the study of the pathway metabolites. We tried to distinguish nicotinic acid, 6-hydroxynicotinic acid and the available derivates by thin layer chromatography, unfortunately with no success. In our Department we

have access to GC-MS (gas chromatograph-mass spectrometer) analytical tools and we started the compound analysis by optimizing the parameters for identification of the available standards (nicotinic acid; 6-hydroxynicotinic acid; 2-hydroxynicotinic acid; 2,5-dihydroxypyridine) (see conference abstracts Rozinka et al. 2015, Bencsik et al. 2015 in the list of project-related publications in the online report).
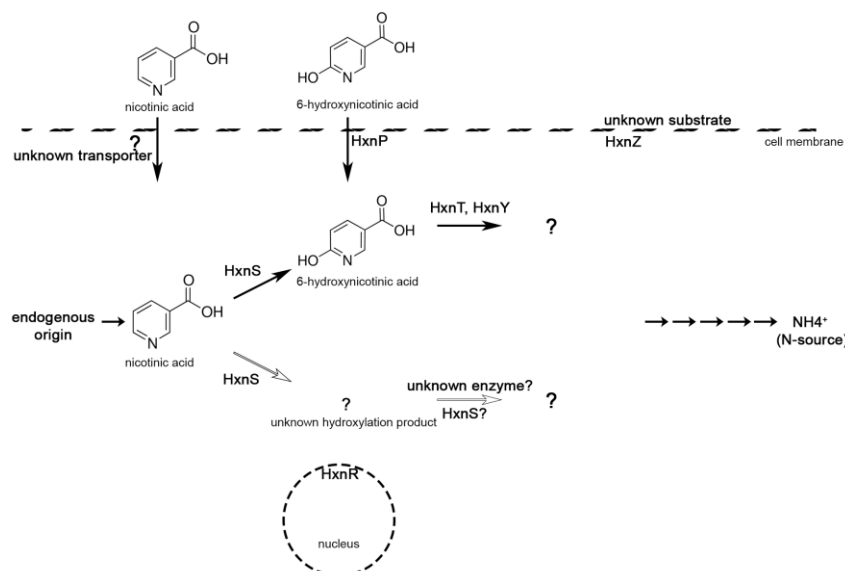
Figure 15. Drawing of the unfurling nicotinic acid utilization pathway.
Solid arrows mark main processes, empty arrows mark the alternative route. Question-marks indicate the yet-unknown details regarding metabolites or protein functions.

Growth test of the transporter deletion mutants *hxnP△* and *hxnZ△* (Fig. 14) revealed only the 6-hydroxynicotinic acid transporter ability of HxnP. Comparing the growth of *hxnP△* on 10 mM 6-hydroxynicotinic acid to that of the parental control strain HZS.185 (Fig. 14) a growth reduction but not a complete lack of growth can be observed in *hxnP△*. This indicates that HxnP is not the exclusive transporter of 6-hydroxynicotinic acid. In the case of *hxnZ△*, we reasoned that it takes part in the transport of a downstream metabolic product, supposing its localization to the cell membrane. In the future we plan to investigate the intracellular localization of HxnP and HxnZ.

2.8. Detailed investigation of the regulation of NDC1 genes

We investigated the induction and repression of the NDC1 genes in details by conducting quantitative Real-Time PCR (qRT-PCR) experiments. The data processing was done by the standard curve method (Larionov *et al.*, 2005). In the first experimental setup we confirmed the expression profile of *hxnS/T/Y/Z/P* genes observed in Northern analysis (Panel A, Fig. 15). The wild type (WT) control (FGSC A26) and *hxnR△* (HZS.136) strains were grown on the neutral acetamide (1 mM) as sole N-source for 8h at 37°C and then the mycelia was transferred to N-source free medium (N-starvation) in one case, a 1 mM acetamide medium supplemented with 1 mM nicotinic acid in the second case and 1 mM acetamide medium supplemented with 1 mM 6-hydroxynicotinic acid in the third case and further incubated for 2h. Results presented in Panel A show that expression of *hxnS/T/Y/Z/P* genes are under the regulation of *hxnR* transcription factor and their expressions can be induced by either nicotinic acid or 6-hydroxynicotinic acid. This result confirms completely the Northern result shown in Fig. 13. In a second experimental setup we investigated the inducibility of nicotinic acid and 6-hydroxynicotinic acid in an *hxB20* mutant (HZS.135). *hxB20* is a non-functional allele of *hxB,* the gene product is the enzyme necessary for the terminal sulphurylation of the molybdenum cofactor in the active site (Amrani *et al.*, 2000), therefore responsible for the activity of HxnS. In this experiment wild type (WT) (FGSC A26), *hxnR△* (HZS.136)*, hxnR constitutive mutant (aplAᶜ7)* (FGSC A872) and *hxB20* (HZS.135) *strains* were grown on 1 mM acetamide for 8h and then the strains were transferred to N-source free medium; acetamide medium supplemented with 1 mM nicotinic acid and acetamide medium supplemented with

1 mM 6-hydroxynicotinic acid and further incubated for 2h. The results shown on Panel B on Figure 15 reveal that nicotinic acid is not the true inducer, it is a downstream metabolite, 6-hydroxynicotinic acid or a further downstream product.
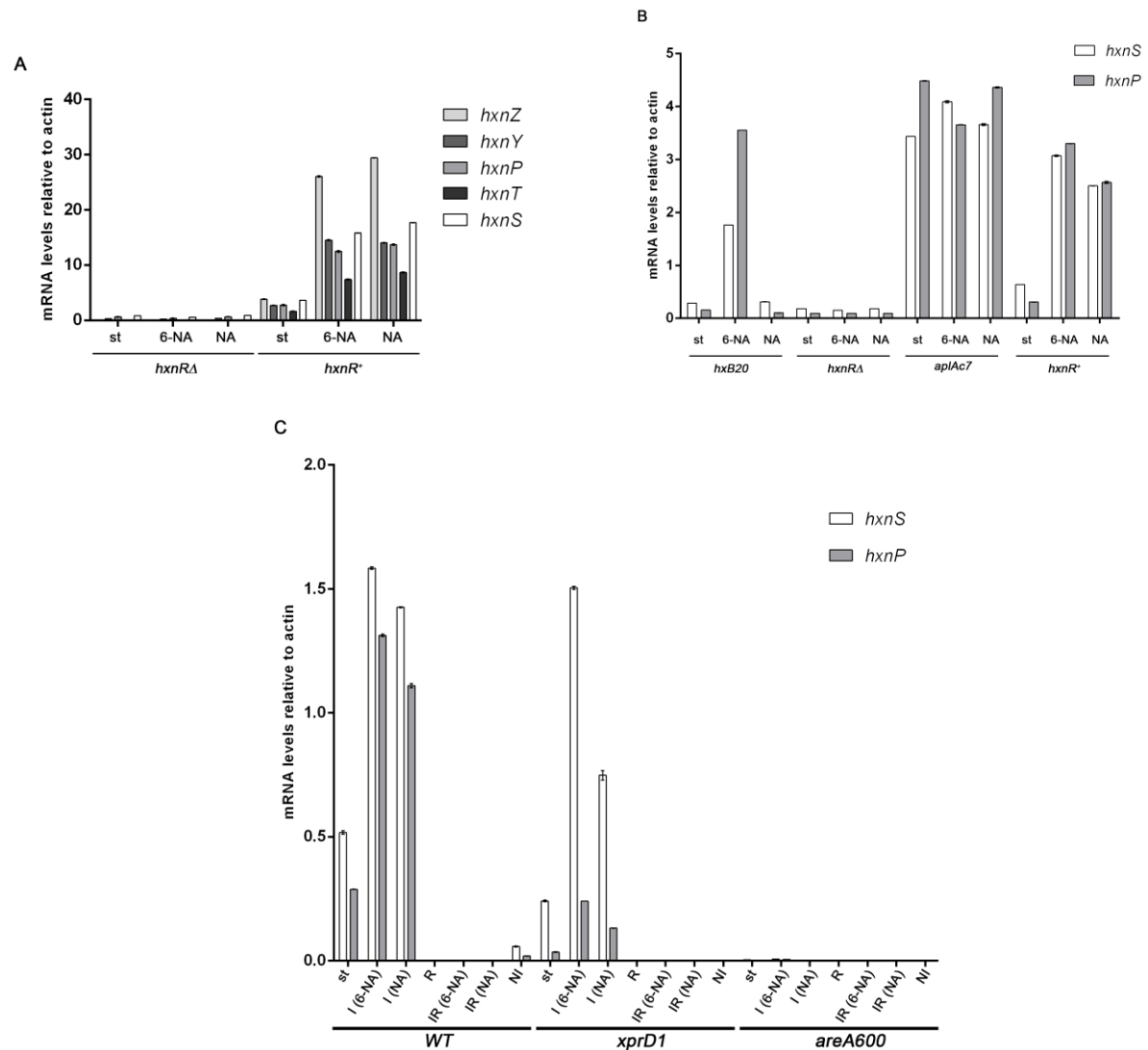
Figure 15. Analysis of NDC1 gene mRNA levels in wild type and various regulatory mutants under N-starved, induced, repressed and induced-repressed conditions.

Panel A. mRNA levels of hxnZ/Y/P/T/S genes in wild type (WT) *hxnR⁺* control (FGSC A26) and *hxnRΔ* mutants (HZS.136). st: N-starvation condition, 6-NA: induced with 6-hydroxynicotinic acid; NA: induced with nicotinic acid (for detailed growth conditions see the text).). qRT-PCR data were processed according to the standard curve method, the housekeeping gene was actin. Standard deviations based on three replicates are shown.

Panel B. mRNA levels of *hxnP* and *hxnS* genes in *hxB20* strain (HZS.135), *hxnRΔ* mutant (HZS.136), *hxnR* constitutive mutant (*aplAc7*) (FGSC A872) and in WT control (FGSC A26) strain. st: N-starvation condition, 6-NA: induced with 6-hydroxynicotinic acid; NA: induced with nicotinic acid (for detailed growth conditions see the text). qRT-PCR data were processed according to the standard curve method, the housekeeping gene was actin. Standard deviations based on three replicates are shown.

Panel C. mRNA levels of *hxnP* and *hxnS* genes in WT control (FGSC A26), *areA* constitutive mutant (*xprD1*) (HZS.216) and *areA* loss-of-function mutant (*areA600*) (CS3095) strains. st: N-starvation condition, I(6-NA): induced with 6-hydroxynicotinic acid; I (NA): induced with nicotinic acid; R: repressed condition (by ammonium); IR (6-NA): induced-repressed condition by supplementing the medium with 6-hydroxynicotinic acid and ammonium; IR (NA): induced-repressed condition by supplementing the medium with nicotinic acid and ammonium; NI: non-induced condition (medium was not supplemented with inducers or repressors)(for detailed growth conditions see the text). qRT-PCR data were processed according to the standard curve method, the housekeeping gene was actin. Standard deviations based on three replicates are shown.

In a third experimental setup we investigated the role of AreA, a general nitrogen metabolic pathway co-regulator (Gomez *et al.*, 2003; Scazzocchio, 2000) and confirmed the repression by ammonium, that was first observed by Northern analysis (Fig. 13). Expression of two representatives of NDC1 genes, *hxnS*

and *hxnP* were monitored in HZS.216, a derepressed mutant of *areA* (*xprD1*) (Kudla *et al.*, 1990) and *areA* loss-of-function mutant (*areA600*) (CS3095). Strains were grown on 5 mM ammonium as sole N-source for 8 h, then the mycelia were transferred to N-source free medium (N-starvation); 10 mM 6-hydroxynicotinic acid as sole N-source (induced condition); 10 mM nicotinic acid as sole N-source (induced condition); 10 mM 6-hydroxynicotinic acid as sole N-source supplemented with 5 mM ammonium (induced-repressed condition); 10 mM nicotinic acid as sole N-source supplemented with 5 mM ammonium (induced-repressed condition) and finally to 1 mM acetamide as sole N-source (non-induced condition). Results shown in Panel C of Fig. 15 confirms that ammonium completely represses *hxnS* and *hxnP*, and AreA can be a co-regulator of HxnR. Notably, in case of *areA* derepression mutant, the expression of *hxnS* is induced similarly that can be seen in the induced wild type strain, while the induction of *hxnP* expression level is less than it is observed in the induced wild type strain, but higher than the basal level of expression in the non-induced wild type and also higher than the N-starved wild type level. The most probable explanation, which can be tested in the future is that the AreA binding sites in the *hxnP* promoter are in close proximity with HxnR binding sites, thus in the AreA derepression mutant the abnormal high concentration of AreA might inhibit the binding of HxnR. In the near future we plan to start an *in silico* analysis about the AreA binding GATA sites on promoter of HxnR and the other NDC1 cluster genes and establish a hypothesis about the co-regulative role of AreA on the expression of the NDC1 cluster genes. An additional result of this experimental setup is that we observed that N-starvation results in a low level of induction of the gene expression of *hxnS* and *hxnP*.

3. Discovery of NDC2 and NDC3 cluster genes

On the basis of transcriptome analysis of our dually localized chromatin associated HmbB deletion mutant (Karacsony *et al.*, 2014) we succesfully predicted the existence of a second cluster (NDC2) and a third cluster (NDC3). The HmbB has role in modulation of nuclear gene expressions especially to those, which take part in metabolism (Karacsony *et al.*, 2015). Transcriptome analysis based on NGS RNAseq data was carried out on wild type and *hmbBΔ* strains under different conditions (growth on 37°C and 42°C, and normal and N-starvation condition) (non-published data). Screening the results to genes which show similar expression pattern to the NDC1 cluster genes and at the same time they clusterize, had led us to a cluster with 3 genes on Chromosome VI (NDC2), 40 kb far from the NDC1 cluster and a cluster with 2 genes on Chromosome I (NDC3). *In silico* analysis of the distribution of the NDC1 genes among fungi revealed that in Pezizomycotina the NDC1 and NDC2 genes are not separated and form a single cluster. Besides these findings, the *A. nidulans* GeneBank transformation experiment, which meant to identify a nicotinic acid non-utilizer mutant allele *hxn6* in strain CS308 (*pyroA4 hxn6 veA1*) (gift from Prof. Scazzocchio), resulted in the identification of a GeneBank plasmid, which complemented the *hxn6* phenotype. Sequence analysis of the GeneBank plasmid revealed a genomic region, which carried all the 3 genes of NDC2 cluster. We named this genes *hxnX*, *hxnW* and *hxnV*. With qRT-PCR analysis we studied the regulation of *hxnX, hxnW* and *hxnV* expression under N-starved and induced conditions in wild type and *hxnRΔ* strains. For details see the section 2.8, first experiment.
The three genes showed the features of those of the pathway genes. Their expression required HxnR and it was inducible by nicotinic acid and 6-hydroxynicotinic acid (Fig. 17).
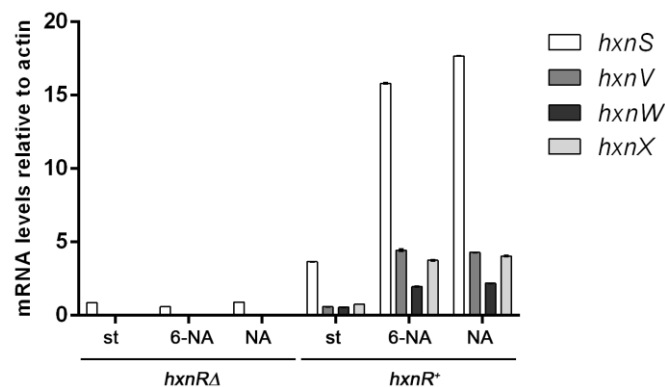
Figure 17. mRNA levels of *hxnV, hxnW, hxnX* and as control, the *hxnS* genes in wild-type *hxnR*[+] control (FGSC A26) and *hxnRΔ* mutants (HZS.136). st: N-starvation condition, 6-NA: induced with 6-hydroxynicotinic acid; NA: induced with nicotinic acid (for detailed growth conditions see the text at section 2.8 for Panel A of Fig. 13).). qRT-PCR data were processed according to the standard curve method, the housekeeping gene was actin. Standard deviations based on three replicates are shown.

Investigation of NDC2 cluster genes has already started in our lab, and the results of growth tests, HxnV purification and phenotypic characterization of the *hxnW* deletion mutan thave been presented on conferences in 2012-2015 (see list of publications related to the project in the online report, Poster abstracts of Ámon et al. and Bokor et al.). We also started to study the two genes in NDC3, which we named *hxnN* and *hxnM*. Our preliminary results on their expression show inducibility by nicotinic acid and dependence on HxnR transcription factor.

Including the preliminary results on NDC2 and NDC3 to the unfurling nicotinic acid utilization pathway, we drew the updated schematic presentation of the pathway (Fig. 18).
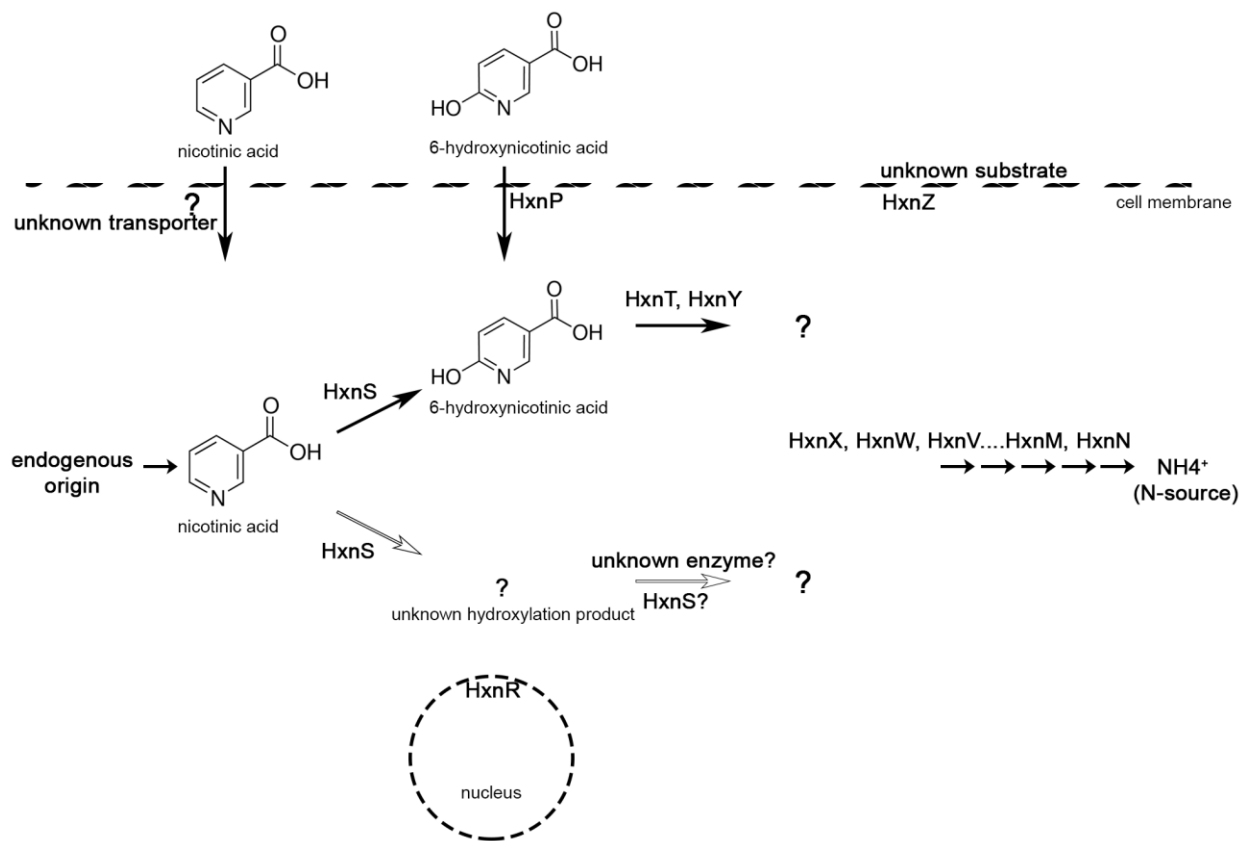
Figure 18. Drawing of the unfurling nicotinic acid utilization pathway including the knowledge on NDC2 and NDC3
Solid arrows mark main processes, empty arrows mark the alternative route. Question-marks indicate the yet-unknown details regarding metabolites or protein functions.

4. References

Alhapel, A., Darley, D. J., Wagener, N., Eckel, E., Elsner, N. & Pierik, A. J. (2006). Molecular and functional analysis of nicotinate catabolism in *Eubacterium barkeri. Proceedings of the National Academy of Sciences of the United States of America* **103**, 12341-12346.

Amrani, L., Primus, J., Glatigny, A., Arcangeli, L., Scazzocchio, C. & Finnerty, V. (2000). Comparison of the sequences of the *Aspergillus nidulans hxB* and *Drosophila melanogaster ma-l* genes with *nifS* from *Azotobacter vinelandii* suggests a mechanism for the insertion of the terminal sulphur atom in the molybdopterin cofactor. *Molecular microbiology* **38**, 114-125.

Cecchetto, G., Richero, M., Oestreicher, N., Muro-Pastor, M. I., Pantano, S. & Scazzocchio, C. (2012). Mutations in the basic loop of the Zn binuclear cluster of the UaY transcriptional activator suppress mutations in the dimerisation domain. *Fungal genetics and biology : FG & B* **49**, 731-743.

Chaveroche, M. K., Ghigo, J. M. & d'Enfert, C. (2000). A rapid method for efficient gene replacement in the filamentous fungus *Aspergillus nidulans*. *Nucleic acids research* **28**, E97.

Cisse, O. H., Almeida, J. M., Fonseca, A., Kumar, A. A., Salojarvi, J., Overmyer, K., Hauser, P. M. & Pagni, M. (2013). Genome sequencing of the plant pathogen *Taphrina deformans*, the causal agent of peach leaf curl. *MBio* **4**, e00055-00013.

Coughlan, M. P., Mehra, R. K., Barber, M. J. & Siegel, L. M. (1984). Optical and electron paramagnetic resonance spectroscopic studies on purine hydroxylase II from *Aspergillus nidulans*. *Arch Biochem Biophys* **229**, 596-603.

Cultrone, A., Scazzocchio, C., Rochet, M., Montero-Moran, G., Drevet, C. & Fernandez-Martin, R. (2005). Convergent evolution of hydroxylation mechanisms in the fungal kingdom: molybdenum cofactor-independent hydroxylation of xanthine via alpha-ketoglutarate-dependent dioxygenases. *Molecular microbiology* **57**, 276-290.

Darlington, A. J. & Scazzocchio, C. (1968). Evidence for an alternative pathway of xanthine oxidation in *Aspergillus nidulans*. *Biochimica et biophysica acta* **166**, 569-571.

Enroth, C., Eger, B. T., Okamoto, K., Nishino, T. & Pai, E. F. (2000). Crystal structures of bovine milk xanthine dehydrogenase and xanthine oxidase: structure-based mechanism of conversion. *Proceedings of the National Academy of Sciences of the United States of America* **97**, 10723-10728.

Ensign, J. C. & Rittenberg, S. C. (1964). The Pathway of Nicotinic Acid Oxidation by a *Bacillus* Species. *The Journal of biological chemistry* **239**, 2285-2291.

Galanopoulou, K., Scazzocchio, C., Galinou, M. E. & other authors (2014). Purine utilization proteins in the Eurotiales: cellular compartmentalization, phylogenetic conservation and divergence. *Fungal genetics and biology : FG & B* **69**, 96-108.

Garattini, E., Fratelli, M. & Terao, M. (2008). Mammalian aldehyde oxidases: genetics, evolution and biochemistry. *Cellular and molecular life sciences : CMLS* **65**, 1019-1048.

Glatigny, A. & Scazzocchio, C. (1995). Cloning and molecular characterization of *hxA*, the gene coding for the xanthine dehydrogenase (purine hydroxylase I) of *Aspergillus nidulans*. *The Journal of biological chemistry* **270**, 3534-3550.

Gomez, D., Garcia, I., Scazzocchio, C. & Cubero, B. (2003). Multiple GATA sites: protein binding and physiological relevance for the regulation of the proline transporter gene of *Aspergillus nidulans*. *Molecular microbiology* **50**, 277-289.

Gournas, C., Oestreicher, N., Amillis, S., Diallinas, G. & Scazzocchio, C. (2011). Completing the purine utilisation pathway of *Aspergillus nidulans*. *Fungal genetics and biology : FG & B* **48**, 840-848.

Hille, R. (2005). Molybdenum-containing hydroxylases. *Arch Biochem Biophys* **433**, 107-116.

Ishikita, H., Eger, B. T., Okamoto, K., Nishino, T. & Pai, E. F. (2012). Protein conformational gating of enzymatic activity in xanthine oxidoreductase. *J Am Chem Soc* **134**, 999-1009.

Jimenez, J. I., Canales, A., Jimenez-Barbero, J., Ginalski, K., Rychlewski, L., Garcia, J. L. & Diaz, E. (2008). Deciphering the genetic determinants for aerobic nicotinic acid degradation: the nic cluster from *Pseudomonas putida* KT2440. *Proceedings of the National Academy of Sciences of the United States of America* **105**, 11329-11334.

Karacsony, Z., Gacser, A., Vagvolgyi, C., Scazzocchio, C. & Hamari, Z. (2014). A dually located multi-HMG-box protein of *Aspergillus nidulans* has a crucial role in conidial and ascospore germination. *Molecular microbiology* **94**, 383-402.

Karacsony, Z., Gacser, A., Vagvolgyi, C. & Hamari, Z. (2015). Further characterization of the role of the mitochondrial high-mobility group box protein in the intracellular redox environment of *Aspergillus nidulans*. *Microbiology* **161**, 1897-1908.

Kudla, B., Caddick, M. X., Langdon, T., Martinez-Rossi, N. M., Bennett, C. F., Sibley, S., Davies, R. W. & Arst, H. N., Jr. (1990). The regulatory gene *areA* mediating nitrogen metabolite repression in *Aspergillus nidulans*. Mutations affecting specificity of gene activation alter a loop residue of a putative zinc finger. *The EMBO journal* **9**, 1355-1364.

Kwon, N. J., Garzia, A., Espeso, E. A., Ugalde, U. & Yu, J. H. (2010). FlbC is a putative nuclear C2H2 transcription factor regulating development in *Aspergillus nidulans*. *Molecular microbiology* **77**, 1203-1219.

Larionov, A., Krause, A. & Miller, W. (2005). A standard curve based method for relative real time PCR data processing. *BMC Bioinformatics* **6**, 62.

Lewis, N. J., Hurt, P., Sealy-Lewis, H. M. & Scazzocchio, C. (1978). The genetic control of the molybdoflavoproteins in *Aspergillus nidulans*. IV. A comparison between purine hydroxylase I and II. *Eur J Biochem* **91**, 311-316.

Mehra, R. K. & Coughlan, M. P. (1989). Characterization of purine hydroxylase I from *Aspergillus nidulans*. *J Gen Microbiol* **135**, 273-278.

Montero-Moran, G. M., Li, M., Rendon-Huerta, E., Jourdan, F., Lowe, D. J., Stumpff-Kane, A. W., Feig, M., Scazzocchio, C. & Hausinger, R. P. (2007). Purification and characterization of the FeII- and alpha-ketoglutarate-dependent xanthine hydroxylase from *Aspergillus nidulans*. *Biochemistry* **46**, 5293-5304.

Nikolaev, I., Cochet, M. F. & Felenbok, B. (2003). Nuclear import of zinc binuclear cluster proteins proceeds through multiple, overlapping transport pathways. *Eukaryotic cell* **2**, 209-221.

Pokorska, A., Drevet, C. & Scazzocchio, C. (2000). The analysis of the transcriptional activator PrnA reveals a tripartite nuclear localisation sequence. *Journal of molecular biology* **298**, 585-596.

Roy, A., Kucukural, A. & Zhang, Y. (2010). I-TASSER: a unified platform for automated protein structure and function prediction. *Nat Protoc* **5**, 725-738.

Scazzocchio, C. (1973). The genetic control of molybdoflavoproteins in *Aspergillus nidulans*. II. Use of NADH dehydrogenase activity associated with xanthine dehydrogenase to investigate substrate and product inductions. *Mol Gen Genet* **125**, 147-155.

Scazzocchio, C., Holl, F. B. & Foguelman, A. I. (1973). The genetic control of molybdoflavoproteins in *Aspergillus nidulans*. Allopurinol-resistant mutants constitutive for xanthine-dehydrogenase. *Eur J Biochem* **36**, 428-445.

Scazzocchio, C., Sdrin, N. & Ong, G. (1982). Positive regulation in a eukaryote, a study of the *uaY* gene of *Aspergillus nidulans*: I. Characterization of alleles, dominance and complementation studies, and a fine structure map of the *uaY--oxpA* cluster. *Genetics* **100**, 185-208.

Scazzocchio, C. (1994). The purine degradation pathway, genetics, biochemistry and regulation. *Prog Ind Microbiol* **29**, 221-257.

Scazzocchio, C. (2000). The fungal GATA factors. *Curr Opin Microbiol* **3**, 126-131.

Sealy-Lewis, H. M., Scazzocchio, C. & Lee, S. (1978). A mutation defective in the xanthine alternative pathway of *Aspergillus nidulans*: its use to investigate the specificity of *uaY* mediated induction. *Mol Gen Genet* **164**, 303-308.

Sealy-Lewis, H. M., Lycan, D. & Scazzocchio, C. (1979). Product induction of purine hydroxylase II in *Asperigillus nidulans*. *Mol Gen Genet* **174**, 105-106.

Suarez, T., de Queiroz, M. V., Oestreicher, N. & Scazzocchio, C. (1995). The sequence and binding specificity of UaY, the specific regulator of the purine utilization pathway in *Aspergillus nidulans*, suggest an evolutionary relationship with the PPR1 protein of *Saccharomyces cerevisiae*. *The EMBO journal* **14**, 1453-1467.

Truglio, J. J., Theis, K., Leimkuhler, S., Rappa, R., Rajagopalan, K. V. & Kisker, C. (2002). Crystal structures of the active and alloxanthine-inhibited forms of xanthine dehydrogenase from *Rhodobacter capsulatus*. *Structure* **10**, 115-125.

Wong, K. H., Hynes, M. J., Todd, R. B. & Davis, M. A. (2009). Deletion and overexpression of the *Aspergillus nidulans* GATA factor AreB reveals unexpected pleiotropy. *Microbiology* **155**, 3868-3880.

Yamaguchi, Y., Matsumura, T., Ichida, K., Okamoto, K. & Nishino, T. (2007). Human xanthine oxidase changes its substrate specificity to aldehyde oxidase type upon mutation of amino acid residues in the active site: roles of active site residues in binding and activation of purine substrate. *J Biochem* **141**, 513-524.

Yu, J. H., Hamari, Z., Han, K. H., Seo, J. A., Reyes-Dominguez, Y. & Scazzocchio, C. (2004). Double-joint PCR: a PCR-based molecular tool for gene manipulations in filamentous fungi. *Fungal genetics and biology : FG & B* **41**, 973-981.

Zhang, Y. (2008). I-TASSER server for protein 3D structure prediction. *BMC Bioinformatics* **9**, 40.